Commun. Theor. Phys. **76** (2024) 075002 (21pp) https://doi.org/10.1088/1572-9494/ad3222

Considering individual game behavior and time delay in the multi-channel rumor propagation model

Yafang Dong[1], **Liang'an Huo**[1,2], **Xiaoxiao Xie**[1] **and Ming Li**[1]

[1] Business School, University of Shanghai for Science and Technology, Shanghai 200093, China
[2] School of Intelligent Emergency Management, University of Shanghai for Science and Technology, Shanghai 200093, China

E-mail: huohuolin@yeah.net

Received 10 November 2023, revised 23 February 2024
Accepted for publication 11 March 2024
Published 3 June 2024

Abstract

The rapid development of the Internet has accelerated the spread of rumors, posing challenges to social cohesion and stability. To address this, a multi-channel rumor propagation model incorporating individual game behavior and time delay is proposed. It depicts individuals strategically choosing propagation channels in the rumor spread process, capturing real-world intricacies more faithfully. Specifically, the model allowing spreaders to choose between text and video information base channels. Strategy adoption hinges on benefits versus costs, with payoffs dictating strategy and the propagation process determining an individual's state. By theoretical analysis of the model, the propagation threshold and equilibrium points are obtained. Then the stability of the model is further demonstrated based on Routh–Hurwitz judgment and Descartes' Rule of Signs. Numerical simulations are conducted to verify the correctness of the theoretical results and the sensitivity of the model to key parameters. The outcomes reveal that increasing the propagation cost of spreaders can significantly curb the spread of rumors. In contrast to the classical *ISR* model, rumors spread faster and more widely in the improved multi-channel rumor propagation model in this paper, which is a feature more aligned with real-world scenarios. Finally, the validity and predictive ability of the model are verified by using real rumor propagation data sets, indicating that the improved multi-channel rumor propagation model has good practical application and predictive value.

Keywords: multi-channel, rumor propagation, time delay, game behavior

(Some figures may appear in colour only in the online journal)

1. Introduction

With the rapid development of the Internet, we have entered the era of universal mobile network interconnection, and the channels of information exchange have also undergone significant changes. On one hand, people no longer just passively obtain information from a single official channel, but can also actively seek information through autonomous internet searches. On the other hand, there are more and more platforms for information dissemination, for example, various social networking software and Internet websites are used by people to express their opinions. By July 2023, the number of people using the Internet had reached 5.19 billion, equivalent to 64.5% of the global population. Of these, the number of active social media users reached 4.88 billion, equivalent to 60.6% of the global population [1]. Nevertheless, due to the inherent anonymity of the internet, the public may not consider the integrity and authenticity of information when posting it. Some individuals may even deliberately propagate rumors or false information for various reasons, which may include personal gain, satisfying their vanity, or achieving certain purposes. There is no doubt that the rampant spread of rumors can harm public safety and social stability [2–6]. To effectively control the spread of rumors in the fast-developing

social media era, it is necessary to deeply understand the new features that appear in the rumor propagation dynamics.

In recent years, many studies have done in-depth research on the theory of rumor transmission in social networks from different perspectives based on disease transmission models, incorporating rumor propagation mechanisms [7–11], language environments [12–14], network topology [15–17], external environmental noise [18–22] and multiplex networks [23, 24]. For example, Wang *et al* consider rumor spreading under the multi-lingual environment, and further establish a new model with cross-transmitted mechanism [25]. Zhang *et al* think that rumor propagation and behavior spreading are usually closely coupled with each other and the interaction will have great influence on the spreading dynamics, so they propose a novel interacting model of rumor propagation and behavior spreading in multiplex networks [26]. Since there is a diffusion-to-reception process in the propagation of information, the resulting time delay is an important and unavoidable factor that affects the dynamic behavior of a network system, which can induce instability, bifurcation and even chaos behavior [27, 28], and therefore some researchers have included time delay in their models [29, 30]. However, the propagation characteristics of different propagation channels are different. Jia *et al* proposed an improved susceptible nodes, infected nodes, recovered nodes (SIR) model to further divide the propagation channels of rumors on social networks into point-to-point propagation and group propagation, and analyzed the difference in rumor propagation in the two propagation channels [31]. Dong *et al* further classified rumor spreading channels into a friendship network propagation channel and a media website propagation channel, and proposed an improved two-layer rumor propagation model to analyze the influence of different propagation channels on the rumor propagation process [32]. Shao *et al* first proposed a three-layer network model with coupled offline and online social networks, and then proposed an improved SIR model to further model the evolution of dynamic processes occurring in multiple interacting network systems, and found that the model has diverse performance compared to the classical multi-layer model [33].

Based on the aforementioned reviews, the most commonly proposed models are based on epidemiological models. However, a significant limitation of these models lies in their disregard for human subjective initiatives in the transmission process [34]. Therefore, some scholars have tried to use game theory to describe human subjective initiative and add it to the study of rumor propagation theory. Xiao *et al* proposed a rumor spreading model considering evolutionary game, anti-rumor information and users' psychological factors, which provides a theoretical basis for studying the intrinsic laws in propagation dynamics [35]. Askarizadeh *et al* proposed an evolutionary game model to analyze the rumor process in social networks, considering the influence of people's decisions on rumor propagation and control [36]. Li *et al* proposed a tripartite cognitive model of information dissemination based on the symbiosis and antagonism of multiple types of messages and the polymorphism of users' cognitive processes under the influence of multiple messages, and the experiments show that the model not only describes the coexistence/confrontation relationship of multiple messages, but it can also perceive the game situation of multiple messages [37].

Indeed, the flourishing development of science and technology has given people more choices of channels to express their views. However, most of the existing studies pay insufficient attention to individuals' preferences when choosing communication channels. The hypothesis of rationality in economic decision making assumes that individuals are rational and act in a manner that maximizes their economic interests. In the era of self-media, online views, clicks, and followers can yield economic gains for the spreaders, but at the same time running a self-media account incurs some costs. Evidently, the process of choosing propagation channels can be explained by a game-like explanatory framework in which individuals typically choose strategies that optimize their payoffs. Based on the above analysis, this paper proposes an improved rumor propagation game model. The model comprehensively considers the effects of multiple communication channels and human behavioral games on the dynamics of rumor propagation. Next, the propagation threshold of the system is obtained and the stability of the equilibria is proved. Then, the correctness of the theoretical analysis is verified by a numerical simulation. Finally, the validity of the model is verified with a real dataset of Twitter.

This paper is organized as follows. In section 2, we detail an improved rumor propagation game model that includes three propagation channels. In section 3, we discuss the existence of boundary equilibria and internal equilibria, and prove the existence of equilibria. In section 4, some numerical simulations are used to support our theoretical analysis. In section 5, the validity of the model is verified with the real dataset of Twitter. Finally, section 6 discusses the conclusions and future work of this paper.

2. Model formulation

Nowadays, a powerful information repository has been created online, containing many forms of data, knowledge and resources [38, 39]. Individuals can easily obtain rich information and services from the information base and have the opportunity to publish information in it. The anonymity of the network provides opportunities for rumors to spread widely in the information base.

Firstly, specifically, the multiple forms of data in the information base provide diverse ways for rumors to be expressed. Through multimedia forms such as text, pictures and videos, rumors can be presented more vividly and attract more attention. For example, on social media, rumors that can be presented in the form of engaging videos will be more likely to attract users' attention, prompting users to share them and thus accelerating their spread. Secondly, expertise in the information base can make rumors appear more authoritative. Rumors often rely on fictional experts or scientific theories to increase their persuasiveness. Real expertise in the information base may be distorted or misused, making

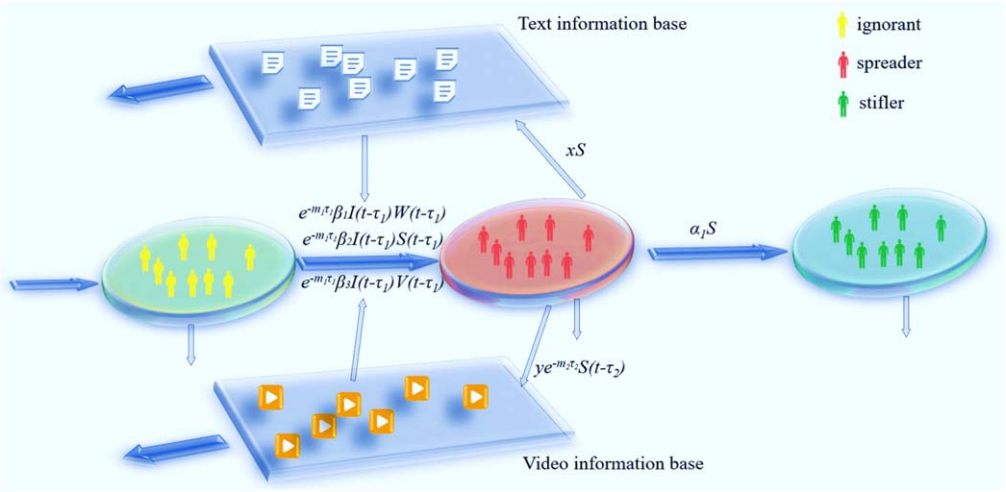

Figure 1. The schematic diagram of rumor propagation process.

the rumor more deceptive. For example, a rumor may claim to be endorsed by a medical expert, creating greater fear among the public. Finally, the anytime, anywhere nature of service of the information bases allows rumors to spread widely in a short period of time. Users can access the information base at any time through mobile devices such as mobile phones and tablets to quickly access and spread rumors. For example, after a rumor is published in an information base, users can immediately share it through social media, creating a rapid chain of information propagation.

Therefore, as an important propagation channel, information bases have an important role in the rumor propagation process that cannot be ignored. In order to deeply elaborate the new features that information bases give to the rumor propagation process, this paper will develop an improved multi-channel model.

Information bases can be further categorized, based on their content, into text information bases and video information bases. Text information base refers to the information collection consisting of information disseminated in the form of text, pictures and links on various social media platforms, WeChat public accounts, forums, news websites, Twitter, etc. Video information base refers to the collection of information disseminated in the form of videos on various video platforms, such as YouTube and TikTok. Therefore, this study further classifies rumor propagation channels into text information base propagation channel, video information base propagation channel, and individual interaction propagation channel. The individual interaction propagation channel refers to rumors spread through interaction, phone calls, text messages, and word-of-mouth. Delineating rumor propagation channels help to understand the characteristics of rumor propagation in different forms and channels, so as to better cope with the spread rumor propagation.

Drawing from the preceding analysis, the model divides the population into three distinct groups based on their varied responses to rumors. Ignorant: people who have never been exposed to rumors (denoted by I). Spreaders: people who know about rumors and propagate them (denoted by S). Stifler: people who know about rumors but do not propagate them (denoted by R). Rumors in text form are denoted by W. Rumors in video form are denoted by V.

Table 1. The meanings of the parameters.

Symbol	Meaning
Λ	The probability of entry
λ	The probability of removal
β_1	The probability of text rumor propagation
β_2	The probability of contact propagation
β_3	The probability of video rumor propagation
m_1	Impact degree of time delay τ_1
m_2	Impact degree of time delay τ_2
τ	The length of the information interval
α_1	The probability of forgetting or losing interest
b	The choice intensity
ε	The individual's sensitivity to information at the current moment
C_w	The cost of posting a text rumor
C_v	The cost of posting a video rumor
p	The imitation intensity
I	The density of the ignorant
S	The density of the spreader
R	The density of the stifler
W	Density of rumors in text form
V	Density of rumors in video form
τ_1	Time required for an ignorant person to receive a message and decide whether to post it or not
τ_2	Time required by the spreader to create a rumor in video form
N	Total number of people

A schematic diagram of the rumor propagation channels is shown in figure 1 and the relevant parameters are defined in detail in table 1.

The propagation rules are established as follows:

(1) An ignorant individual I can be exposed to a rumor through three different channels. The first channel is the text information base propagation channel. The probability

that an individual receives a rumor through this channel and subsequently propagates the rumor is denoted as β_1. The second channel is the individual interaction propagation channel. The probability that an individual receives and propagates a rumor through this channel is denoted as β_2. The third channel is the video information base propagation channel. The probability that an individual receives and propagates a rumor through this channel is denoted as β_3.

(2) A spreader S will propagate rumors through three propagation channels. Posting rumors in text information base, posting rumors in video information base, and interacting with others to propagate rumors. Spreaders S will choose which propagation channel to utilize for maximizing their own benefits by evaluating their potential gains.

(3) The spreader S is transformed into a stifler R by forgetting or losing interest in propagating the rumor with a certain probability α_1.

(4) The ignorant I who receives a message takes time to decide whether to post it or not. This period of time causes a delay in the transformation of the individual's state, denoted by τ_1. In addition, the spreader S spends some time in creating the rumor in video form, and the delay caused by this period of time is denoted by τ_2.

(5) Individuals enter the community at a rate of Λ and move out of the community at a rate of λ. Rumors in text form and rumors in video form move out of the information base at a rate of λ.

According to the hypothesis of rational humans, to maximize their profit, spreaders will consider the benefits and corresponding costs of each strategy when propagating rumors, so as to choose the optimal propagation strategy. This decision making process can be regarded as a game process, in which the spreader needs to choose between propagation and non-propagation to maximize their payoff. This decision making process can be formalized as a game theory model. Specifically, the spreader can be considered as a game participant, and propagation and non-propagation as two alternative strategies for this participant. At the same time, the audience group can be considered as another player whose response can influence the benefits of the spreader. In this model, the expected payoff to a spreader for converting a rumor into text form and posting it to a text information base is denoted by g_w, the benefits (including the attention and reputation received after propagating the rumor) that can be derived from the strategy is denoted by Q_w and the corresponding costs (including the time cost, the risk of blocking and the risk of reputation damage) are denoted by C_w. Similarly, the expected payoff to a spreader for converting a rumor into video form and posting it to a text information base is denoted by g_v, the benefits (including the attention and reputation received after propagating the rumor) that can be derived from the strategy are denoted by Q_v, and the corresponding costs (including the time cost, the risk of blocking and the risk of reputation damage) are denoted by C_v.

$$g_w = Q_w(I, W) - C_w, \tag{1}$$

$$g_v = Q_v(I, V) - C_v, \tag{2}$$

where $Q_w(I, W) = \mathrm{e}^{-m_1\tau_1}\beta_1 NIW$ and $Q_v(I, V) = \mathrm{e}^{-m_1\tau_1}\beta_3 NIV$. Specifically, when a spreader chooses the strategy of propagating rumors through the text information base channel, the probability that an ignorant come into contact with a rumor in the text information base and successfully transform into a spreader is denoted as $\beta_1 IW$. Consequently, under this strategy, the total number of individuals transforming from the ignorant to spreaders is represented as $\beta_1 NIW$. Considering the time delay factor, this transformation quantity is further expressed as $\mathrm{e}^{-m_1\tau_1}\beta_1 NIW$. In this paper, we consider this transformation quantity as the benefit of the spreader's choice of this strategy, i.e., the exposure and influence that the spreader gains.

Similarly, when a spreader chooses the strategy of propagating through the video information base channel, the probability that an ignorant come into contact with a rumor in the video information base and successfully transform into spreaders is denoted as $\beta_2 IV$. Therefore, under this strategy, the total transformation quantity is $\beta_2 NIV$. Considering the time delay factor, this transformation quantity is further expressed as $\mathrm{e}^{-m_1\tau_1}\beta_2 NIV$. This transformation quantity is considered to be the benefit of the spreader's choice of this strategy, i.e., the exposure and influence gained by the spreader. It is more realistic to assume that individuals make decisions by combining payoff at the current moment and payoff in the past period.

$$M_1(t) = \varepsilon g_w(t) + \int_{t-\tau}^{t} g_w(\eta)\alpha \mathrm{e}^{\alpha(t-\eta)}\mathrm{d}\eta, \tag{3}$$

$$M_2(t) = \varepsilon g_v(t) + \int_{t-\tau}^{t} g_v(\eta)\alpha \mathrm{e}^{\alpha(t-\eta)}\mathrm{d}\eta, \tag{4}$$

where τ denotes the length of time that an individual considers the payoff when choosing a strategy and ε reflects the individual's sensitivity to the payoff at the current moment. When $\varepsilon = 0$, it indicates that individuals only consider the payoff of past periods when choosing strategies; when $\tau = 0$, it indicates that individuals are only influenced by the payoff at the current moment when choosing strategies. In addition, an exponentially decaying memory function $K(t) = \alpha \mathrm{e}^{-\alpha t}$ is used to characterize the effect of information accumulated over time on spreaders' communication decisions. The decision payoff matrix of spreaders is shown in table 2.

Obviously, whether an individual chooses the information base channel to spread rumors depends on the final payoff function. Therefore, combined with the Fermi function [40], the rate at which an individual changes strategy is assumed to be a nonlinear response function to the final payoff function.

$$P(W \leftarrow S) = \frac{a}{1 + \mathrm{e}^{-bM_1(t)}} - \frac{a}{2}, \tag{5}$$

$$P(V \leftarrow S) = \frac{a}{1 + \mathrm{e}^{-bM_2(t)}} - \frac{a}{2}, \tag{6}$$

where b is the choice intensity. A larger b indicates that the individual is more sensitive to payoff and more rational, even if the difference between the expected payoff of the two

strategies is small [41]. Let $p = av_0$ denote the imitation intensity factor, where v_0 represents the rate at which one individual is linked to another or the information base, and a represents the degree of influence. When $M_1(t) > 0$, i.e., when the final payoff of choosing the text information base dissemination strategy is positive, the spreaders are likely to choose this channel to propagate rumors. And the larger $M_1(t)$ is, the higher the probability of choosing this channel. When $M_1(t) < 0$, i.e., when the final payoff of choosing the text information base dissemination strategy is negative, the spreaders will not choose this channel to spread rumors according to the rational man assumption. When $M_1(t) = 0$, individuals do not change their strategy. Similarly, the decision process of whether a spreader chooses the video information base propagation channel strategy is also divided into these three categories. According to the above analysis, the proportion x of spreaders choosing the text information base propagation channel strategy and the proportion y of spreaders choosing the video information base propagation channel strategy satisfy the differential equation shown below [42].

$$\frac{\mathrm{d}x}{\mathrm{d}t} = px(1-x)\left(\frac{1}{1+\mathrm{e}^{-bM_1(t)}} - \frac{1}{2}\right), \tag{7}$$

$$\frac{\mathrm{d}y}{\mathrm{d}t} = py(1-y)\left(\frac{1}{1+\mathrm{e}^{-bM_2(t)}} - \frac{1}{2}\right). \tag{8}$$

According to the above rumor propagation rules and the game behavior analysis of the channel selection by the spreader, the following is the mean field equation of the multi-channel rumor propagation model constructed in this paper,

$$\begin{cases} \dfrac{\mathrm{d}I(t)}{\mathrm{d}t} = \Lambda - \beta_1 I(t)W(t) \\ \quad - \beta_2 I(t)S(t) - \beta_3 I(t)V(t) - \lambda I(t), \\ \dfrac{\mathrm{d}S(t)}{\mathrm{d}t} = \mathrm{e}^{-m_1\tau_1}\beta_1 I(t-\tau_1)W(t-\tau_1) \\ \quad + \mathrm{e}^{-m_1\tau_1}\beta_2 I(t-\tau_1)S(t-\tau_1) \\ \quad + \mathrm{e}^{-m_1\tau_1}\beta_3 I(t-\tau_1)V(t-\tau_1) \\ \quad -\alpha_1 S(t) - \lambda S(t), \\ \dfrac{\mathrm{d}R(t)}{\mathrm{d}t} = \alpha_1 S(t) - \lambda R(t), \\ \dfrac{\mathrm{d}W(t)}{\mathrm{d}t} = xS(t) - \lambda W(t), \\ \dfrac{\mathrm{d}V(t)}{\mathrm{d}t} = y\mathrm{e}^{-m_2\tau_2}S(t-\tau_2) - \lambda V(t), \\ \dfrac{\mathrm{d}x(t)}{\mathrm{d}t} = px(1-x)\left(\dfrac{1}{1+\mathrm{e}^{-bM_1(t)}} - \dfrac{1}{2}\right), \\ \dfrac{\mathrm{d}y(t)}{\mathrm{d}t} = py(1-y)\left(\dfrac{1}{1+\mathrm{e}^{-bM_2(t)}} - \dfrac{1}{2}\right), \\ M_1(t) = \varepsilon g_w(t) + \displaystyle\int_{t-\tau}^{t} g_w(\eta)\alpha\mathrm{e}^{\alpha(t-\eta)}\mathrm{d}\eta, \\ M_2(t) = \varepsilon g_v(t) + \displaystyle\int_{t-\tau}^{t} g_v(\eta)\alpha\mathrm{e}^{\alpha(t-\eta)}\mathrm{d}\eta. \end{cases} \tag{9}$$

Table 2. The payoff matrix.

Strategy/type	Rumor in the text information base	Rumor in the video information base
Propagate	M_1	M_2
Non-propagate	0	0

3. Model analysis

3.1. Equilibria and threshold

In this section, the system (9) will be analyzed theoretically. Firstly, we use the next generation matrix method to find the basic regeneration number of the system (9). Subsequently, we get the boundary equilibrium point and the internal equilibrium point of the system. Finally, we further analyze the stability of the equilibrium points.

Considering the practical implications of x, y, the system exists in the following three cases. When $x = 0$ and $y = 0$, the system (9) always has a rumor-free equilibrium point $E_1^0 = \left(\frac{\Lambda}{\lambda}, 0, 0, 0, 0, 0, 0\right)$. When $x = 1$, $y = 0$, the system (9) always has a rumor-free equilibrium point $E_2^0 = \left(\frac{\Lambda}{\lambda}, 0, 0, 0, 0, 1, 0\right)$. When $x = 0$, $y = 1$, the system (9) always has a rumor-free equilibrium point $E_3^0 = \left(\frac{\Lambda}{\lambda}, 0, 0, 0, 0, 0, 1\right)$. Further using the next generation matrix method, the corresponding basic regeneration number is $R_0 = \dfrac{\beta_2\Lambda}{\lambda(\alpha_1+\lambda)\mathrm{e}^{m_1\tau_1}}$. Then, define $R_1 = \dfrac{(\beta_1+\beta_2\lambda)\Lambda}{\lambda^2(\alpha_1+\lambda)\mathrm{e}^{m_1\tau_1}}$ and $R_2 = \dfrac{(\beta_3\mathrm{e}^{-m_2\tau_2}+\beta_2\lambda)\Lambda}{\lambda^2(\alpha_1+\lambda)\mathrm{e}^{m_1\tau_1}}$.

Next, we analyze the other possible equilibrium points in the system (9) in the three cases mentioned above. When $S \neq 0$, there exist three corresponding rumor-prevailing equilibrium points.

$$\begin{aligned} E_4^* &= (I_4^*, S_4^*, R_4^*, W_4^*, V_4^*, x_4^*, y_4^*) \\ &= \left(\frac{(\alpha_1+\lambda)\mathrm{e}^{m_1\tau_1}}{\beta_2}, \frac{\beta_2\Lambda - \lambda(\alpha_1+\lambda)\mathrm{e}^{m_1\tau_1}}{\beta_2(\alpha_1+\lambda)\mathrm{e}^{m_1\tau_1}}, \frac{\alpha_1 S_4^*}{\lambda}, 0, 0, 0, 0\right), \\ E_5^* &= (I_5^*, S_5^*, R_5^*, W_5^*, V_5^*, x_5^*, y_5^*) \\ &= \left(\frac{\lambda(\alpha_1+\lambda)\mathrm{e}^{m_1\tau_1}}{\beta_1+\beta_2\lambda}, \frac{(\beta_1+\beta_2\lambda)\Lambda - \lambda^2(\alpha_1+\lambda)\mathrm{e}^{m_1\tau_1}}{(\beta_1+\beta_2\lambda)(\alpha_1+\lambda)\mathrm{e}^{m_1\tau_1}}, \right. \\ &\quad \left. \frac{\alpha_1 S_5^*}{\lambda}, \frac{S_5^*}{\lambda}, 0, 1, 0\right), \\ E_6^* &= (I_6^*, S_6^*, R_6^*, W_6^*, V_6^*, x_6^*, y_6^*) \\ &= \left(\frac{\lambda(\alpha_1+\lambda)\mathrm{e}^{m_1\tau_1+m_2\tau_2}}{\beta_3+\beta_2\lambda\mathrm{e}^{m_2\tau_2}}, \right. \\ &\quad \frac{(\beta_3+\beta_2\lambda\mathrm{e}^{m_2\tau_2})\Lambda - \lambda^2(\alpha_1+\lambda)\mathrm{e}^{m_1\tau_1+m_2\tau_2}}{(\beta_3+\beta_2\lambda\mathrm{e}^{m_2\tau_2})(\alpha_1+\lambda)\mathrm{e}^{m_1\tau_1}}, \\ &\quad \left. \frac{\alpha_1 S_6^*}{\lambda}, 0, \frac{S_6^*}{\lambda\mathrm{e}^{m_2\tau_2}}, 0, 1\right). \end{aligned}$$

The above six are the boundary equilibrium points, and the following is to consider whether there is an internal equilibrium point. Let the right end of each equation in system (9) be 0, we can obtain

$$\begin{cases} \Lambda - \beta_1 I(t)W(t) - \beta_2 I(t)S(t) \\ - \beta_3 I(t)V(t) - \lambda I(t) = 0, \\ \mathrm{e}^{-m_1\tau_1}\beta_1 I(t-\tau_1)W(t-\tau_1) \\ + \mathrm{e}^{-m_1\tau_1}\beta_2 I(t-\tau_1)S(t-\tau_1) \\ + \mathrm{e}^{-m_1\tau_1}\beta_3 I(t-\tau_1)V(t-\tau_1) \\ - \alpha_1 S(t) - \lambda S(t) = 0, \\ \alpha_1 S(t) - \lambda R(t) = 0, \\ xS(t) - \lambda W(t) = 0, \\ y\mathrm{e}^{-m_2\tau_2}S(t-\tau_2) - \lambda V(t) = 0, \\ px(1-x)\left(\dfrac{1}{1+\mathrm{e}^{-bM_1(t)}} - \dfrac{1}{2}\right) = 0, \\ py(1-y)\left(\dfrac{1}{1+\mathrm{e}^{-bM_2(t)}} - \dfrac{1}{2}\right) = 0, \\ \varepsilon g_w(t) + \displaystyle\int_{t-\tau}^{t} g_w(\eta)\alpha\mathrm{e}^{\alpha(t-\eta)}\mathrm{d}\eta = 0, \\ \varepsilon g_v(t) + \displaystyle\int_{t-\tau}^{t} g_v(\eta)\alpha\mathrm{e}^{\alpha(t-\eta)}\mathrm{d}\eta = 0. \end{cases} \tag{10}$$

Then, the internal equilibrium point $E_7^* = (I_7^*, S_7^*, R_7^*, W_7^*, V_7^*, x_7^*, y_7^*)$ is obtained, where $I_7^* = \dfrac{\Lambda - (\alpha_1+\lambda)\mathrm{e}^{m_1\tau_1}S_7^*}{\lambda}$, $R_7^* = \dfrac{\alpha_1 S_7^*}{\lambda}$, $W_7^* = \dfrac{C_w\mathrm{e}^{m_1\tau_1}\lambda}{\beta_1 N(\Lambda - (\alpha_1+\lambda)\mathrm{e}^{m_1\tau_1}S_7^*)}$, $V_7^* = \dfrac{C_v\mathrm{e}^{m_1\tau_1}\lambda}{\beta_3 N(\Lambda - (\alpha_1+\lambda)\mathrm{e}^{m_1\tau_1}S_7^*)}$, $x_7^* = \dfrac{C_w\mathrm{e}^{m_1\tau_1}\lambda^2}{\beta_1 N(\Lambda - (\alpha_1+\lambda)\mathrm{e}^{m_1\tau_1}S_7^*)S_7^*}$, $y_7^* = \dfrac{C_v\mathrm{e}^{m_1\tau_1+m_2\tau_2}\lambda^2}{\beta_3 N(\Lambda - (\alpha_1+\lambda)\mathrm{e}^{m_1\tau_1}S_7^*)S_7^*}$, $E_7^* = (I_7^*, S_7^*, R_7^*, W_7^*, V_7^*, x_7^*, y_7^*)$ exists if and only if $S_5^* \in \left(0, \dfrac{\Lambda}{(\alpha_1+\lambda)\mathrm{e}^{m_1\tau_1}}\right]$.

Theorem 1. $E_7^* = (I_7^*, S_7^*, R_7^*, W_7^*, V_7^*, x_7^*, y_7^*)$ exists if, and only if, $S_7^* \in \left(0, \dfrac{\Lambda}{(\alpha_1+\lambda)\mathrm{e}^{m_1\tau_1}}\right]$.

Proof. From system (10) it follows that

$$\frac{(C_w+C_v)\mathrm{e}^{m_1\tau_1}}{N} + \beta_2 S^* \frac{\Lambda - (\alpha_1+\lambda)\mathrm{e}^{m_1\tau_1}S^*}{\lambda} - \mathrm{e}^{m_1\tau_1}(\alpha_1+\lambda)S^* = 0. \tag{11}$$

Denote

$$G(S) = \frac{(C_w+C_v)\mathrm{e}^{m_1\tau_1}}{N} + \beta_2 S\frac{\Lambda - (\alpha_1+\lambda)\mathrm{e}^{m_1\tau_1}S}{\lambda} - \mathrm{e}^{m_1\tau_1}(\alpha_1+\lambda)S. \tag{12}$$

It is easy to know that the zero of equation (12) in the range $S^* \in \left(0, \dfrac{\Lambda}{(\alpha_1+\lambda)\mathrm{e}^{m_1\tau_1}}\right]$ is the rumor-prevailing equilibrium of system (10). Obviously, $G(0) = \dfrac{(C_w+C_v)\mathrm{e}^{m_1\tau_1}}{N}$.

$$G'(S) = \beta_2\frac{\Lambda - (\alpha_1+\lambda)\mathrm{e}^{m_1\tau_1}S}{\lambda} - \beta_2 S\frac{(\alpha_1+\lambda)\mathrm{e}^{m_1\tau_1}}{\lambda} - \mathrm{e}^{m_1\tau_1}(\alpha_1+\lambda), \tag{13}$$

when $S = 0$

$$\begin{aligned} G'(0) &= \beta_2 \frac{\Lambda}{\lambda} - \mathrm{e}^{m_1\tau_1}(\alpha_1 + \lambda) \\ &= \mathrm{e}^{m_1\tau_1}(\alpha_1 + \lambda)\left[\frac{\beta_2\Lambda}{\lambda(\alpha_1 + \lambda)\mathrm{e}^{m_1\tau_1}} - 1\right] \\ &= \mathrm{e}^{m_1\tau_1}(\alpha_1 + \lambda)[R_1^0 - 1] \end{aligned} \tag{14}$$

and

$$G\left(\frac{\Lambda}{(\alpha_1 + \lambda)\mathrm{e}^{m_1\tau_1}}\right) = \frac{(C_w + C_v)\mathrm{e}^{m_1\tau_1}}{N} - \Lambda. \tag{15}$$

From equations (13)–(15), there exists an S^* in the interval $\left(0, \frac{\Lambda}{(\alpha_1 + \lambda)\mathrm{e}^{m_1\tau_1}}\right]$ when $R_0 > 1$ and $\Lambda > \frac{(C_w + C_v)\mathrm{e}^{m_1\tau_1}}{N}$. At this point $G(S^*) = 0$.

Then, we prove the uniqueness of S^*. From equation (11), we can get $\beta_2 \frac{\Lambda - (\alpha_1 + \lambda)\mathrm{e}^{m_1\tau_1}S^*}{\lambda} - \mathrm{e}^{m_1\tau_1}(\alpha_1 + \lambda) < 0$. Then we have

$$\begin{aligned} G'(S^*) &= \beta_2 \frac{\Lambda - (\alpha_1 + \lambda)\mathrm{e}^{m_1\tau_1}S^*}{\lambda} \\ &- \beta_2 S^* \frac{(\alpha_1 + \lambda)\mathrm{e}^{m_1\tau_1}}{\lambda} - \mathrm{e}^{m_1\tau_1}(\alpha_1 + \lambda) < 0. \end{aligned} \tag{16}$$

It is easy to obtain that G is strictly decreasing at each of its zeros. If there exists another rumor-prevailing equilibrium point S_1^* excepts S^* satisfies that $G'(S_1^*) \geqslant 0$, which leads to a contradiction.

Then, we analyze the local stability of the above equilibria when $\tau \geqslant 0$. Let $E_n = (I_n, S_n, R_n, W_n, V_n, x_n, y_n)$, denote the equilibrium point of the system, and for the sake of analysis, let

$$\begin{aligned} P_0(n) &= (\mathrm{e}^{-m_1\tau_1}\beta_1 N I_n W_n - C_w)(1 + \varepsilon - \mathrm{e}^{-\alpha\tau}), \\ P_1(n) &= (\mathrm{e}^{-m_1\tau_1}\beta_3 N I_n V_n - C_v)(1 + \varepsilon - \mathrm{e}^{-\alpha\tau}). \end{aligned} \tag{17}$$

3.2. Stability of rumor equilibria

Linearizing the system near the equilibrium point and still expressing the linearized system as an equation with respect to (I, S, R, W, V, x, y):

$$\begin{cases} \dfrac{\mathrm{d}I}{\mathrm{d}t} = -(\beta_1 W_n + \beta_2 S_n + \beta_3 V_n + \lambda)I - \beta_2 I_n S - \beta_1 I_n W - \beta_3 I_n V, \\ \dfrac{\mathrm{d}S}{\mathrm{d}t} = \mathrm{e}^{-m_1\tau_1}(\beta_1 W_n + \beta_2 S_n + \beta_3 V_n)I + (\mathrm{e}^{-m_1\tau_1}\beta_2 I_n - \alpha_1 - \lambda)S \\ + \mathrm{e}^{-m_1\tau_1}\beta_1 I_n W + \mathrm{e}^{-m_1\tau_1}\beta_3 I_n V, \\ \dfrac{\mathrm{d}R}{\mathrm{d}t} = \alpha_1 S - \lambda R, \\ \dfrac{\mathrm{d}W}{\mathrm{d}t} = x_n S - \lambda W + S_n x, \\ \dfrac{\mathrm{d}V}{\mathrm{d}t} = \mathrm{e}^{-m_2\tau_2}y_n S - \lambda V + \mathrm{e}^{-m_2\tau_2}S_n y, \\ \dfrac{\mathrm{d}x}{\mathrm{d}t} = T_1(n)\left[\varepsilon I + \displaystyle\int_{t-\tau}^{t} I(\eta)\alpha\mathrm{e}^{-\alpha(t-\eta)})\mathrm{d}\eta\right] \\ + T_2(n)\left[\varepsilon W + \displaystyle\int_{t-\tau}^{t} W(\eta)\alpha\mathrm{e}^{-\alpha(t-\eta)})\mathrm{d}\eta\right] + T_3(n)x, \\ \dfrac{\mathrm{d}y}{\mathrm{d}t} = T_4(n)\left[\varepsilon I + \displaystyle\int_{t-\tau}^{t} I(\eta)\alpha\mathrm{e}^{-\alpha(t-\eta)})\mathrm{d}\eta\right] \\ + T_5(n)\left[\varepsilon V + \displaystyle\int_{t-\tau}^{t} V(\eta)\alpha\mathrm{e}^{-\alpha(t-\eta)})\mathrm{d}\eta\right] + T_6(n)y, \end{cases} \tag{18}$$

where

$$T_1(n) = px_n(1 - x_n)\frac{b\mathrm{e}^{-bP_0(n)}}{(1 + \mathrm{e}^{-bP_0(n)})^2}(\mathrm{e}^{-m_1\tau_1}\beta_1 NW_n),$$
$$T_2(n) = px_n(1 - x_n)\frac{b\mathrm{e}^{-bP_0(n)}}{(1 + \mathrm{e}^{-bP_0(n)})^2}(\mathrm{e}^{-m_1\tau_1}\beta_1 NI_n),$$

$$T_3(n) = p(1 - 2x_n)\left(\frac{1}{1 + \mathrm{e}^{-bP_0(n)}} - \frac{1}{2}\right),$$
$$T_4(n) = py_n(1 - y_n)\frac{b\mathrm{e}^{-bP_1(n)}}{(1 + \mathrm{e}^{-bP_1(n)})^2}(\mathrm{e}^{-m_1\tau_1}\beta_3 NV_n),$$

$$T_5(n) = py_n(1 - y_n)\frac{b\mathrm{e}^{-bP_1(n)}}{(1 + \mathrm{e}^{-bP_1(n)})^2}(\mathrm{e}^{-m_1\tau_1}\beta_3 NI_n),$$
$$T_6(n) = p(1 - 2y_n)\left(\frac{1}{1 + \mathrm{e}^{-bP_1(n)}} - \frac{1}{2}\right).$$

Let $(I, S, R, W, V, x, y) = \mathrm{e}^{\mu t}(h_1, h_2, h_3, h_4, h_5, h_6, h_7)$ be an exponential solution of the linearized system, where μ and h are constants, bring them into the linear system and use $\int_{t-\tau}^{t} h_i\mathrm{e}^{-\mu\eta}\alpha\mathrm{e}^{-\alpha(t-\eta)}\mathrm{d}\eta = \frac{\alpha(1 - \mathrm{e}^{-(\mu+\alpha)\tau})h_i\mathrm{e}^{-\mu\eta}}{\mu + \alpha}$. Then the characteristic equation can be obtained by calculating,

$$\begin{vmatrix} Q_1(n) - \theta & \beta_2 I_n & 0 & -\beta_1 I_n & -\beta_3 I_n & 0 & 0 \\ Q_2(n) & Q_3(n) - \theta & 0 & \mathrm{e}^{-m_1\tau_1}\beta_1 I_n & \mathrm{e}^{-m_1\tau_1}\beta_3 I_n & 0 & 0 \\ 0 & \alpha_1 & -\lambda - \theta & 0 & 0 & 0 & 0 \\ 0 & x_n & 0 & -\lambda - \theta & 0 & S_n & 0 \\ 0 & \mathrm{e}^{-m_2\tau_2}y_n & 0 & 0 & -\lambda - \theta & 0 & \mathrm{e}^{-m_2\tau_2}S_n \\ Q_4(n) & 0 & 0 & Q_5(n) & 0 & Q_6(n) - \theta & 0 \\ Q_7(n) & 0 & 0 & 0 & Q_8(n) & 0 & Q_9(n) - \theta \end{vmatrix} = 0, \tag{19}$$

where

$$Q_1(n) = -(\beta_1 W_n + \beta_2 S_n + \beta_3 V_n + \lambda),$$
$$Q_2(n) = \mathrm{e}^{-m_1\tau_1}(\beta_1 W_n + \beta_2 S_n + \beta_3 V_n),$$
$$Q_3(n) = (\mathrm{e}^{-m_1\tau_1}\beta_2 I_n - \alpha_1 - \lambda),$$

$$Q_4(n) = px_n(1 - x_n)\frac{b\mathrm{e}^{-bP_0(n)}}{(1 + \mathrm{e}^{-bP_0(n)})^2}(\mathrm{e}^{-m_1\tau_1}\beta_1 NW_n)$$
$$\times\left[\varepsilon + \frac{\alpha(1 - \mathrm{e}^{-(\mu+\alpha)\tau})}{\mu + \alpha}\right],$$
$$Q_5(n) = px_n(1 - x_n)\frac{b\mathrm{e}^{-bP_0(n)}}{(1 + \mathrm{e}^{-bP_0(n)})^2}(\mathrm{e}^{-m_1\tau_1}\beta_1 NI_n)$$
$$\times\left[\varepsilon + \frac{\alpha(1 - \mathrm{e}^{-(\mu+\alpha)\tau})}{\mu + \alpha}\right],$$
$$Q_6(n) = p(1 - 2x_n)\left(\frac{1}{1 + \mathrm{e}^{-bP_0(n)}} - \frac{1}{2}\right),$$

$$Q_7(n) = py_n(1 - y_n)\frac{be^{-bP_1(n)}}{(1 + e^{-bP_1(n)})^2}(e^{-m_1\tau_1}\beta_3 NV_n)$$
$$\times\left[\varepsilon + \frac{\alpha(1 - e^{-(\mu+\alpha)\tau})}{\mu + \alpha}\right],$$
$$Q_8(n) = py_n(1 - y_n)\frac{be^{-bP_1(n)}}{(1 + e^{-bP_1(n)})^2}(e^{-m_1\tau_1}\beta_3 NI_n)$$
$$\times\left[\varepsilon + \frac{\alpha(1 - e^{-(\mu+\alpha)\tau})}{\mu + \alpha}\right],$$
$$Q_9(n) = p(1 - 2y_n)\left(\frac{1}{1 + e^{-bP_1(n)}} - \frac{1}{2}\right).$$

Theorem 2. The stability of the boundary equilibria of the system is as follows:

(1) When $R_0 < 1$, the rumor-free equilibrium point E_1^0 is locally asymptotically stable.
(2) The rumor-free equilibrium points E_2^0, E_3^0 and E_4^* are always unstable.
(3) When $C_w < \frac{\beta_1 N\Lambda e^{-m_1\tau_1}}{\beta_1 + \beta_2\lambda}\left(1 - \frac{1}{R_1}\right)$, the rumor-prevailing equilibrium point E_5^* is locally asymptotically stable.
(4) When $C_v < \frac{\beta_3 N\Lambda e^{-m_1\tau_1}}{\beta_3 + \beta_2\lambda e^{m_2\tau_2}}\left(1 - \frac{1}{R_2}\right)$, $R_2 > 1$, and $\lambda I_6^* < \Lambda$, the rumor epidemic equilibrium point E_6^* is locally asymptotically stable.

Proof. (1) Firstly, we analyze the equilibrium point $E_1^0 = \left(\frac{\Lambda}{\lambda}, 0, 0, 0, 0, 0, 0\right)$ and bring it into equation (12) to get its corresponding characteristic equation

$$\begin{vmatrix} -\lambda-\theta & \frac{\beta_2\Lambda}{\lambda} & 0 & -\frac{\beta_1\Lambda}{\lambda} & -\frac{\beta_3\Lambda}{\lambda} & 0 & 0 \\ 0 & Q_3(1)-\theta & 0 & e^{-m_1\tau_1}\frac{\beta_1\Lambda}{\lambda} & e^{-m_1\tau_1}\frac{\beta_3\Lambda}{\lambda} & 0 & 0 \\ 0 & \alpha_1 & -\lambda-\theta & 0 & 0 & 0 & 0 \\ 0 & 0 & 0 & -\lambda-\theta & 0 & 0 & 0 \\ 0 & 0 & 0 & 0 & -\lambda-\theta & 0 & 0 \\ 0 & 0 & 0 & 0 & 0 & Q_6(1)-\theta & 0 \\ 0 & 0 & 0 & 0 & 0 & 0 & Q_9(1)-\theta \end{vmatrix} = 0. \quad (20)$$

It is easy to obtain that the characteristic roots of the above equation satisfy the following relation:

$$\theta_1 = \theta_2 = \theta_3 = \theta_4 = -\lambda < 0,$$
$$\theta_5 = p\left(\frac{1}{1 + e^{-bc_w(1+\varepsilon-e^{-\alpha\tau})}} - \frac{1}{2}\right) < 0,$$
$$\theta_6 = p\left(\frac{1}{1 + e^{-bc_w(1+\varepsilon-e^{-\alpha\tau})}} - \frac{1}{2}\right) < 0,$$

when $R_1 < 1$, $\theta_7 = -\frac{\lambda(\alpha_1 + \lambda)e^{m_1\tau_1} - \beta_2\Lambda}{\lambda e^{m_1\tau_1}} < 0$.

That is, E_1^0 is locally asymptotically stable.

(2) For the equilibrium point E_2^0, its corresponding characteristic equation is

$$\begin{vmatrix} -\lambda-\theta & \frac{\beta_2\Lambda}{\lambda} & 0 & -\frac{\beta_1\Lambda}{\lambda} & -\frac{\beta_3\Lambda}{\lambda} & 0 & 0 \\ 0 & Q_3(2)-\theta & 0 & e^{-m_1\tau_1}\frac{\beta_1\Lambda}{\lambda} & e^{-m_1\tau_1}\frac{\beta_3\Lambda}{\lambda} & 0 & 0 \\ 0 & \alpha_1 & -\lambda-\theta & 0 & 0 & 0 & 0 \\ 0 & 1 & 0 & -\lambda-\theta & 0 & 0 & 0 \\ 0 & 0 & 0 & 0 & -\lambda-\theta & 0 & 0 \\ 0 & 0 & 0 & 0 & 0 & Q_6(2)-\theta & 0 \\ 0 & 0 & 0 & 0 & 0 & 0 & Q_9(2)-\theta \end{vmatrix} = 0. \quad (21)$$

It is easy to obtain that the above equation has characteristic roots $\theta_1 = -p\left(\frac{1}{1+\mathrm{e}^{-bc_w(1+\varepsilon-\mathrm{e}^{-\alpha\tau})}} - \frac{1}{2}\right) > 0$, so the equilibrium point E_2^0 is unstable.

(3) For the equilibrium point E_3^0, its corresponding characteristic equation is

$$\begin{vmatrix} -\lambda-\theta & \frac{\beta_2\Lambda}{\lambda} & 0 & -\frac{\beta_1\Lambda}{\lambda} & -\frac{\beta_3\Lambda}{\lambda} & 0 & 0 \\ 0 & Q_3(3)-\theta & 0 & \mathrm{e}^{-m_1\tau_1}\frac{\beta_1\Lambda}{\lambda} & \mathrm{e}^{-m_1\tau_1}\frac{\beta_3\Lambda}{\lambda} & 0 & 0 \\ 0 & \alpha_1 & -\lambda-\theta & 0 & 0 & 0 & 0 \\ 0 & 0 & 0 & -\lambda-\theta & 0 & 0 & 0 \\ 0 & \mathrm{e}^{-m_2\tau_2} & 0 & 0 & -\lambda-\theta & 0 & 0 \\ 0 & 0 & 0 & 0 & 0 & Q_6(3)-\theta & 0 \\ 0 & 0 & 0 & 0 & 0 & 0 & Q_9(3)-\theta \end{vmatrix} = 0. \tag{22}$$

It is easy to obtain that the above equation has characteristic roots $\theta_1 = -p\left(\frac{1}{1+\mathrm{e}^{-bc_v(1+\varepsilon-\mathrm{e}^{-\alpha\tau})}} - \frac{1}{2}\right) > 0$, so the equilibrium point E_2^0 is unstable.

(4) For the equilibrium point E_4^*, its corresponding characteristic equation is

$$\begin{vmatrix} Q_1(4)-\theta & (\alpha_1+\lambda)\mathrm{e}^{m_1\tau_1} & 0 & -\beta_1\frac{(\alpha_1+\lambda)\mathrm{e}^{m_1\tau_1}}{\beta_2} & -\beta_3\frac{(\alpha_1+\lambda)\mathrm{e}^{m_1\tau_1}}{\beta_2} & 0 & 0 \\ Q_2(4) & -\theta & 0 & \beta_1\frac{(\alpha_1+\lambda)}{\beta_2} & \beta_3\frac{(\alpha_1+\lambda)}{\beta_2} & 0 & 0 \\ 0 & \alpha_1 & -\lambda-\theta & 0 & 0 & 0 & 0 \\ 0 & 0 & 0 & -\lambda-\theta & 0 & \frac{\beta_2\Lambda-\lambda(\alpha_1+\lambda)\mathrm{e}^{m_1\tau_1}}{\beta_2(\alpha_1+\lambda)\mathrm{e}^{m_1\tau_1}} & 0 \\ 0 & 0 & 0 & 0 & -\lambda-\theta & 0 & \frac{\beta_2\Lambda-\lambda(\alpha_1+\lambda)\mathrm{e}^{m_1\tau_1}}{\beta_2(\alpha_1+\lambda)\mathrm{e}^{m_1\tau_1+m_2\tau_2}} \\ 0 & 0 & 0 & 0 & 0 & Q_6(4)-\theta & 0 \\ 0 & 0 & 0 & 0 & 0 & 0 & Q_9(4)-\theta \end{vmatrix} = 0. \tag{23}$$

$$\begin{aligned} Q_1(4) &= -\frac{\beta_2\Lambda}{(\alpha_1+\lambda)\mathrm{e}^{m_1\tau_1}} - 2\lambda, \\ Q_2(4) &= \frac{\beta_2\Lambda}{(\alpha_1+\lambda)\mathrm{e}^{2m_1\tau_1}} - \frac{\lambda}{\mathrm{e}^{m_1\tau_1}}, \end{aligned}$$

$$\begin{aligned} Q_6(4) &= p\left(\frac{1}{1+\mathrm{e}^{bC_w(1+\varepsilon-\mathrm{e}^{-\alpha\tau})}} - \frac{1}{2}\right), \\ Q_9(4) &= p\left(\frac{1}{1+\mathrm{e}^{bC_v(1+\varepsilon-\mathrm{e}^{-\alpha\tau})}} - \frac{1}{2}\right). \end{aligned}$$

It is easy to obtain that the above equation has characteristic roots $\theta_1 = \beta_2 - 2\lambda^2\mathrm{e}^{m_1\tau_1} - \frac{\alpha_1\lambda}{\alpha_1+\lambda} + \sqrt{Q_{10}} > 0$, where

$$\begin{aligned} Q_{10} &= 4\mathrm{e}^{m_1\tau_1}\alpha_1^2\beta_2\Lambda \\ &+ 4\mathrm{e}^{m_1\tau_1}\alpha_1\lambda\beta_2\Lambda + \beta_2^2\Lambda^2 \\ &- 4\mathrm{e}^{2m_1\tau_1}\alpha_1^3\lambda - 8\mathrm{e}^{2m_1\tau_1}\alpha_1^2\lambda^2 \\ &- 4\mathrm{e}^{2m_1\tau_1}\alpha_1\lambda^3. \end{aligned}$$

So the equilibrium point E_4^* is unstable.

(5) For the equilibrium point E_5^*, its corresponding characteristic equation is

$$\begin{vmatrix} Q_1(5)-\theta & \beta_2 I_5^* & 0 & -\beta_1 I_5^* & -\beta_3 I_5^* & 0 & 0 \\ Q_2(5) & Q_3(5)-\theta & 0 & \mathrm{e}^{-m_1\tau_1}\beta_1 I_5^* & \mathrm{e}^{-m_1\tau_1}\beta_3 I_5^* & 0 & 0 \\ 0 & \alpha_1 & -\lambda-\theta & 0 & 0 & 0 & 0 \\ 0 & 1 & 0 & -\lambda-\theta & 0 & S^* & 0 \\ 0 & 0 & 0 & 0 & -\lambda-\theta & 0 & \mathrm{e}^{-m_2\tau_2}S_5^* \\ 0 & 0 & 0 & 0 & 0 & Q_6(5)-\theta & 0 \\ 0 & 0 & 0 & 0 & 0 & 0 & Q_9(5)-\theta \end{vmatrix} = 0. \tag{24}$$

$$\begin{aligned} Q_1(5) &= -\left(\beta_1\frac{S_5^*}{\lambda}+\beta_2 S_5^*+\lambda\right), \\ Q_2(5) &= \mathrm{e}^{-m_1\tau_1}\left(\beta_1\frac{S_5^*}{\lambda}+\beta_2 S_5^*\right), \\ Q_3(5) &= \beta_2\frac{\lambda(\alpha_1+\lambda)}{\beta_1+\beta_2\lambda}-\alpha_1-\lambda, \\ Q_6(5) &= -p\left(\frac{1}{1+\mathrm{e}^{-bP_0(5)}}-\frac{1}{2}\right), \\ Q_9(5) &= p\left(\frac{1}{1+\mathrm{e}^{-bP_1(5)}}-\frac{1}{2}\right). \end{aligned}$$

where

$$\begin{aligned} P_0(5) &= \left(\frac{\beta_1 N\Lambda\mathrm{e}^{-m_1\tau_1}}{\beta_1+\beta_2\lambda}\left(1-\frac{1}{R_2^0}\right)-C_w\right) \\ &\times(1+\varepsilon-\mathrm{e}^{-\alpha\tau}),\ P_1(5) = -C_v(1+\varepsilon-\mathrm{e}^{-\alpha\tau}). \end{aligned} \tag{25}$$

It is easy to obtain that the characteristic roots of the above equation satisfy the following relation,

$$\begin{aligned} &\theta_1=\theta_2=\theta_3=-\lambda<0, \\ &\theta_4 = p\left(\frac{1}{1+e^{-bc_v(1+\varepsilon-\mathrm{e}^{-\alpha\tau})}}-\frac{1}{2}\right)<0, \end{aligned}$$

$$\theta_5 = -\frac{\beta_1^2\Lambda+\beta_1\lambda^3\mathrm{e}^{m_1\tau_1}+\beta_2^2\lambda\Lambda+2\alpha_1\beta_1\lambda^2\mathrm{e}^{m_1\tau_1}+\alpha_1^2\beta_1\lambda\mathrm{e}^{m_1\tau_1}+2\beta_1\beta_2\lambda\Lambda+\sqrt{Q_{11}}}{2(\beta_2\lambda^3\mathrm{e}^{m_1\tau_1}+\beta_1\lambda^2\mathrm{e}^{m_1\tau_1}+\alpha_1\beta_1\lambda\mathrm{e}^{m_1\tau_1}+\alpha_1\beta_2\lambda^2\mathrm{e}^{m_1\tau_1})}<0,$$

$$\theta_6 = -\frac{\beta_1^2\Lambda+\beta_1\lambda^3\mathrm{e}^{m_1\tau_1}+\beta_2^2\lambda\Lambda+2\alpha_1\beta_1\lambda^2\mathrm{e}^{m_1\tau_1}+\alpha_1^2\beta_1\lambda\mathrm{e}^{m_1\tau_1}+2\beta_1\beta_2\lambda\Lambda-\sqrt{Q_{11}}}{2(\beta_2\lambda^3\mathrm{e}^{m_1\tau_1}+\beta_1\lambda^2\mathrm{e}^{m_1\tau_1}+\alpha_1\beta_1\lambda\mathrm{e}^{m_1\tau_1}+\alpha_1\beta_2\lambda^2\mathrm{e}^{m_1\tau_1})}<0,$$

where

$$\begin{aligned} Q_{11} &= \alpha_1^4\beta_1^2\lambda^2\mathrm{e}^{2m_1\tau_1}-4\alpha_1^3\beta_2^2\lambda^5\mathrm{e}^{2m_1\tau_1} \\ &+8\alpha_1^3\beta_1^2\lambda^3\mathrm{e}^{2m_1\tau_1}+4\alpha_1^2\beta_2^3\lambda^4\Lambda\mathrm{e}^{m_1\tau_1} \\ &+6\alpha_1^2\beta_1\beta_2^2\lambda^3\Lambda\mathrm{e}^{m_1\tau_1} \\ &-12\alpha_1^2\beta_2^2\lambda^6\mathrm{e}^{2m_1\tau_1}-2\alpha_1^2\beta_1^3\lambda\Lambda\mathrm{e}^{m_1\tau_1} \\ &+18\alpha_1^2\beta_1^2\lambda^4\mathrm{e}^{2m_1\tau_1}+8\alpha_1\beta_2^3\lambda^5\Lambda\mathrm{e}^{m_1\tau_1} \\ &+12\alpha_1\beta_1\beta_2^2\lambda^4\Lambda\mathrm{e}^{m_1\tau_1} \\ &-12\alpha_1\beta_2^2\lambda^7\mathrm{e}^{2m_1\tau_1}-4\alpha_1\beta_1^3\lambda^2\Lambda\mathrm{e}^{m_1\tau_1} \\ &+16\alpha_1\beta_1^2\lambda^5\mathrm{e}^{2m_1\tau_1}+\beta_2^4\lambda^4\Lambda^2+4\beta_1\beta_2^3\lambda^3\Lambda^2 \\ &+4\beta_2^3\lambda^6\Lambda\mathrm{e}^{m_1\tau_1}+6\beta_1^2\beta_2^2\lambda^2\Lambda^2 \end{aligned}$$

$$
\begin{aligned}
&+ 6\beta_1\beta_2^2\lambda^5\Lambda e^{m_1\tau_1} - 4\beta_2^2\lambda^8 e^{2m_1\tau_1}\\
&+ 4\beta_1^3\beta_2\lambda\Lambda^2 + \beta_1^4\Lambda^2\\
&- 2\beta_1^3\lambda^3\Lambda e^{m_1\tau_1} + 5\beta_1^2\lambda^6 e^{2m_1\tau_1},
\end{aligned}
$$

when $C_w < \dfrac{\beta_1 N\Lambda e^{-m_1\tau_1}}{\beta_1+\beta_2\lambda}\left(1-\dfrac{1}{R_2^0}\right)$, $\theta_7 = -p\left(\dfrac{1}{1+e^{-bP_0(5)}}-\dfrac{1}{2}\right) < 0$.

Thus E_5^* is locally asymptotically stable.

(6) For the equilibrium point E_6^*, its corresponding characteristic equation is

$$
\begin{vmatrix}
Q_1(6)-\theta & \beta_2 I_6^* & 0 & -\beta_1 I_6^* & -\beta_3 I_6^* & 0 & 0\\
Q_2(6) & Q_3(6)-\theta & 0 & e^{-m_1\tau_1}\beta_1 I_6^* & e^{-m_1\tau_1}\beta_3 I_6^* & 0 & 0\\
0 & \alpha_1 & -\lambda-\theta & 0 & 0 & 0 & 0\\
0 & 0 & 0 & -\lambda-\theta & 0 & S_6^* & 0\\
0 & e^{-m_2\tau_2} & 0 & 0 & -\lambda-\theta & 0 & e^{-m_2\tau_2}S_6^*\\
0 & 0 & 0 & 0 & 0 & Q_6(6)-\theta & 0\\
0 & 0 & 0 & 0 & 0 & 0 & Q_9(6)-\theta
\end{vmatrix} = 0, \tag{26}
$$

where

$$
\begin{aligned}
Q_1(6) &= -\left(\beta_2 S_6^* + \frac{\beta_3 S_6^*}{e^{m_2\tau_2}\lambda} + \lambda\right)\\
&= -\frac{(\beta_3+\beta_2\lambda e^{m_2\tau_2})\Lambda}{(\alpha_1+\lambda)\lambda e^{m_1\tau_1+m_2\tau_2}},\\
Q_2(6) &= e^{-m_1\tau_1}\left(\beta_2 S_6^* + \frac{\beta_3 S_6^*}{e^{m_2\tau_2}\lambda}\right),
\end{aligned}
$$

$$
\begin{aligned}
Q_3(6) &= \left(\frac{\beta_2\lambda(\alpha_1+\lambda)e^{m_2\tau_2}}{\beta_3+\beta_2\lambda e^{m_2\tau_2}} - \alpha_1 - \lambda\right),\\
Q_6(6) &= p\left(\frac{1}{1+e^{-bP_0(6)}}-\frac{1}{2}\right),\\
Q_9(6) &= -p\left(\frac{1}{1+e^{-bP_1(6)}}-\frac{1}{2}\right),
\end{aligned}
$$

$$
\begin{aligned}
P_0(6) &= -C_w(1+\varepsilon-e^{-\alpha\tau}),\\
P_1(6) &= \left(\frac{\beta_3 N\Lambda e^{-m_1\tau_1}}{\beta_3+\beta_2\lambda e^{m_2\tau_2}}\left(1-\frac{1}{R_3^0}\right) - C_v\right)(1+\varepsilon-e^{-\alpha\tau}).
\end{aligned}
$$

It is easy to obtain that the characteristic roots of the above equation satisfy the following relation, $\theta_1=\theta_2=-\lambda<0$, $\theta_3 = p\left(\dfrac{1}{1+e^{-bc_w(1+\varepsilon-e^{-\alpha\tau})}}-\dfrac{1}{2}\right)<0$, when $C_v < \dfrac{\beta_3 N\Lambda e^{-m_1\tau_1}}{\beta_3+\beta_2\lambda e^{m_2\tau_2}}\left(1-\dfrac{1}{R_3^0}\right)$, we have $\theta_4 = -p\left(\dfrac{1}{1+e^{-bP_1(6)}}-\dfrac{1}{2}\right)<0$.

θ_5, θ_6 and θ_7 satisfy the following equation

$$
\begin{aligned}
&a_1\theta^3 + a_2\theta^2 + a_3\theta + a_4 = 0,\\
&a_1 = -1,\\
&a_2 = Q_1 + Q_3 - \lambda,\\
&a_3 = \lambda(Q_1+Q_3) + e^{-m_1\tau_1-m_2\tau_2}\beta_3 I_6^*\\
&- Q_1Q_3 - Q_2\beta_2 I_6^*,\\
&a_4 = -Q_1 e^{-m_1\tau_1-m_2\tau_2}\beta_3 I_6^* - Q_2 e^{-m_2\tau_2}\beta_3 I_6^*\\
&- \lambda Q_1Q_3 - \lambda Q_2\beta_2 I_6^*.
\end{aligned}
$$

When $R_2 > 1$, we have $a_2 < 0$. When $\lambda I_6^* < \Lambda$, we have $a_3 < 0$. According to Descartes' Rule of Sign, the equation $a_1\theta^3 + a_2\theta^2 + a_3\theta + a_4 = 0$ has three negative roots and no positive roots if the above conditions are met. Therefore E_6^* is locally asymptotically stable.

Theorem 3. The internal equilibrium point E_7^* of system (9) is unstable.

Proof. The corresponding characteristic equation of the system at the equilibrium point E_7^* is

$$\begin{vmatrix} Q_1(7)-\theta & \beta_2 I_7^* & 0 & -\beta_1 I_7^* & -\beta_3 I_7^* & 0 & 0 \\ Q_2(7) & Q_3(7)-\theta & 0 & e^{-m_1\tau_1}\beta_1 I_7^* & e^{-m_1\tau_1}\beta_3 I_7^* & 0 & 0 \\ 0 & \alpha_1 & -\lambda-\theta & 0 & 0 & 0 & 0 \\ 0 & x_7 & 0 & -\lambda-\theta & 0 & S_7^* & 0 \\ 0 & e^{-m_2\tau_2}y_7 & 0 & 0 & -\lambda-\theta & 0 & e^{-m_2\tau_2}S_7^* \\ Q_4(7) & 0 & 0 & Q_5(7) & 0 & -\theta & 0 \\ Q_7(7) & 0 & 0 & 0 & Q_8(7) & 0 & -\theta \end{vmatrix} = 0, \tag{27}$$

where

$$\begin{aligned} Q_1(7) &= -(\beta_1 W_7^* + \beta_2 S_7^* + \beta_3 V_7^* + \lambda), \\ Q_2(7) &= e^{-m_1\tau_1}(\beta_1 W_7^* + \beta_2 S_7^* + \beta_3 V_7^*), \\ Q_3(7) &= e^{-m_1\tau_1}\beta_2 I_7^* - \alpha_1 - \lambda, \end{aligned}$$

$$\begin{aligned} Q_4(7) &= \frac{p x_7^*(1-x_7^*)e^{-m_1\tau_1}\beta_1 N W_7^* b}{4} \\ &\times\left[\varepsilon + \frac{\alpha(1-e^{-(\mu+\alpha)\tau})}{\mu+\alpha}\right], \\ Q_5(7) &= \frac{p x_7^*(1-x_7^*)e^{-m_1\tau_1}\beta_1 N I_7^* b}{4} \\ &\times\left[\varepsilon + \frac{\alpha(1-e^{-(\mu+\alpha)\tau})}{\mu+\alpha}\right], \end{aligned}$$

$$\begin{aligned} Q_7(7) &= \frac{p y_7^*(1-y_7^*)e^{-m_1\tau_1}\beta_3 N V_7^* b}{4} \\ &\times\left[\varepsilon + \frac{\alpha(1-e^{-(\mu+\alpha)\tau})}{\mu+\alpha}\right], \\ Q_8(7) &= \frac{p y_7^*(1-y_7^*)e^{-m_1\tau_1}\beta_3 N I_7^* b}{4} \\ &\times\left[\varepsilon + \frac{\alpha(1-e^{-(\mu+\alpha)\tau})}{\mu+\alpha}\right], \end{aligned}$$

which is equivalent to

$$\begin{aligned} &a_0\theta^7 + a_1\theta^6 + a_2\theta^5 + a_3\theta^4 + a_4\theta^3 \\ &+ a_5\theta^2 + a_6\theta + a_7 = 0, \end{aligned} \tag{28}$$

with

$$\begin{aligned} a_0 &= 1 > 0, \\ a_1 &= -Q_1 - 3\lambda e^{m_1\tau_1+m_2\tau_2} + Q_3 e^{m_1\tau_1+m_2\tau_2} < 0, \\ a_2 &= -I_7^* y_7^* \beta_3 e^{-m_1\tau_1-m_2\tau_2} + 3\lambda^2 - Q_8 S_7^* e^{-m_2\tau_2} \\ &+ Q_1 Q_3 - I_7^* x_7^* \beta_1 e^{-m_1\tau_1} - 3(Q_1+Q_3)\lambda - Q_5 S_7^*, \\ a_3 &= \lambda^3 + Q_1 I_7^* y_7^* \beta_3 e^{-m_1\tau_1-m_2\tau_2} + Q_1 Q_8 S_7^* e^{-m_2\tau_2} \\ &+ Q_3 Q_8 S_7^* e^{-m_2\tau_2} - 2\lambda I_7^* y_7^* \beta_3 e^{-m_1\tau_1-m_2\tau_2} - 2Q_8\lambda S_7^* e^{-m_2\tau_2} \\ &- 3(Q_1+Q_3)\lambda^2 + Q_1\beta_1 I_7^* x_7^* e^{-m_1\tau_1} + Q_7\beta_3 I_7^* S_7^* e^{-m_2\tau_2} \\ &+ Q_2\beta_3 I_7^* y_7^* e^{-m_2\tau_2} + 3Q_1Q_3 - 2\beta_1\lambda I_7^* x_7^* e^{-m_1\tau_1} \\ &+ Q_1 Q_5 S_7^* - Q_3 Q_5 S_7^* - 2Q_5\lambda S_7^* - 3Q_2\beta_2\lambda I_7^* \\ &+ Q_4\beta_1 I_7^* S_7^* + Q_2\beta_1 I_7^* x_7^*, \end{aligned}$$

$$\begin{aligned} a_4 &= Q_5 Q_8 S_7^{*2} e^{-m_2\tau_2} - \lambda^2 I_7^* y_7^* \beta_3 e^{-m_1\tau_1-m_2\tau_2} \\ &- Q_8\lambda^2 S_7^{*2} e^{-m_2\tau_2} - (Q_1+Q_3)\lambda + 3Q_1Q_3\lambda^2 \\ &-\beta_1\lambda^2 I_7^* x_7^* e^{-m_1\tau_1} - Q_5\lambda^2 S_7^* - Q_1 Q_3 Q_8 S_7^* e^{-m_2\tau_2} \\ &+Q_8\beta_1 I_7^* S_7^* x_7^* e^{-m_1\tau_1-m_2\tau_2} + 2Q_1\lambda I_7^* y_7^* \beta_3 e^{-m_1\tau_1-m_2\tau_2} \\ &+ Q_5 I_7^* S_7^* y_7^* \beta_3 e^{-m_1\tau_1-m_2\tau_2} \\ &+ 2(Q_1+Q_3)Q_8\lambda S_7^{*2} e^{-m_2\tau_2} - Q_7\beta_2 I_7^{*2} S_7^* \beta_3 e^{-m_1\tau_1-m_2\tau_2} \\ &+ 2Q_1\beta_1\lambda I_7^* x_7^* e^{-m_1\tau_1} - Q_1 Q_3 Q_5 S_7^* \\ &+ 2Q_7\lambda\beta_3 I_7^* S_7^* e^{-m_2\tau_2} + 2Q_2\lambda\beta_3 I_7^* y_7^* e^{-m_2\tau_2} \\ &+ 2(Q_1+Q_3)Q_5\lambda S_7^* - Q_4\beta_1\beta_2 I_7^{*2} S_7^* e^{-m_1\tau_1} \\ &- 3Q_2\lambda^2\beta_3 I_7^* + Q_2 Q_8\beta_2 I_7^* S_7^* e^{-m_2\tau_2} \\ &-Q_3 Q_7\beta_3 I_7^* S_7^* e^{-m_2\tau_2} + Q_2 Q_5\beta_2 I_7^* S_7^* - Q_3 Q_4\beta_1 I_7^* S_7^* \\ &+ 2Q_4\beta_1\lambda I_7^* S_7^* + 2Q_2\beta_1\lambda I_7^* x_7^*, \end{aligned}$$

$$\begin{aligned} a_5 &= Q_1 Q_3\lambda^2 - (Q_1+Q_3)Q_5 Q_8 S_7^{*2} e^{-m_2\tau_2} \\ &+ Q_1\lambda^2 I_7^* y_7^* \beta_3 e^{-m_1\tau_1-m_2\tau_2} + (Q_1+Q_3)Q_8\lambda^2 S_7^* e^{-m_2\tau_2} \\ &+ Q_5 Q_8 S_7^{*2} e^{-m_2\tau_2} - 2Q_7\beta_2\beta_3\lambda I_7^{*2} S_7^* \\ &- Q_4 Q_8\beta_1 I_7^* S_7^{*2} e^{-m_2\tau_2} - Q_5 Q_7\beta_3 I_7^* S_7^{*2} e^{-m_2\tau_2} \\ &+ (Q_1+Q_3)Q_5\lambda^2 S_7^* - Q_2\beta_2\lambda^3 I_7^* \\ &- Q_1 Q_8\beta_1 I_7^* S_7^* x_7^* e^{-m_1\tau_1-m_2\tau_2} - Q_1 Q_5\beta_3 I_7^* S_7^* y_7^* e^{-m_1\tau_1-m_2\tau_2} \\ &- 2Q_1 Q_3 Q_8\lambda S_7^* e^{-m_2\tau_2} + Q_8\beta_1\lambda I_7^* S_7^* x_7^* \\ &+ Q_5\beta_3\lambda I_7^* S_7^* y_7^* + Q_4\beta_1\lambda^2 I_7^* S_7^* + Q_2\beta_1\lambda^2 I_7^* x_7^* \\ &+2Q_2 Q_8\lambda\beta_2 I_7^* S_7^* e^{-m_2\tau_2} - Q_2 Q_8\beta_1 I_7^* S_7^* x_7^* e^{-m_2\tau_2} \\ &- 2Q_3 Q_7\lambda\beta_3 I_7^* S_7^* e^{-m_2\tau_2} - Q_2 Q_5\beta_3 I_7^* S_7^* y_7^* e^{-m_2\tau_2} \\ &-2Q_1 Q_3 Q_5\lambda S_7^* - 2Q_4\beta_1\beta_2\lambda I_7^{*2} S_7^* e^{-m_1\tau_1} \\ &+ 2Q_2 Q_5\lambda\beta_2 I_7^* S_7^* - 2Q_3 Q_4\lambda\beta_1 I_7^* S_7^*, \end{aligned}$$

$$\begin{aligned} a_6 &= Q_1 Q_3 Q_8\lambda S_7^* e^{-m_2\tau_2} - Q_1 Q_3 Q_5 Q_8 S_7^{*2} e^{-m_2\tau_2} \\ &+ Q_1 Q_5 Q_8\lambda S_7^{*2} e^{-m_2\tau_2} + Q_3 Q_5 Q_8\lambda S_7^{*2} e^{-m_2\tau_2} \\ &+ Q_4 Q_8\beta_1\beta_2 I_7^{*2} S_7^{*2} e^{-m_1\tau_1-m_2\tau_2} \\ &- Q_5 Q_7\beta_2\beta_3 I_7^{*2} S_7^{*2} e^{-m_1\tau_1-m_2\tau_2} \\ &+ Q_7\beta_2\beta_3\lambda^2 I_7^{*2} S_7^* e^{-m_1\tau_1-m_2\tau_2} \\ &+ Q_4\beta_1\beta_2\lambda^2 I_7^{*2} S_7^* e^{-m_1\tau_1} \\ &+ Q_1 Q_8\lambda\beta_1 I_7^* S_7^* x_7^* e^{-m_1\tau_1-m_2\tau_2} \\ &+ Q_1 Q_5\beta_3\lambda I_7^* S_7^* y_7^* e^{-m_1\tau_1-m_2\tau_2} \\ &+ Q_2 Q_5 Q_8\beta_2 I_7^* S_7^{*2} e^{-m_2\tau_2} \\ &- Q_3 Q_4 Q_8\beta_1 I_7^* S_7^{*2} e^{-m_2\tau_2} \\ &- Q_2 Q_8\beta_2\lambda^2 I_7^* S_7^* e^{-m_2\tau_2} \end{aligned}$$

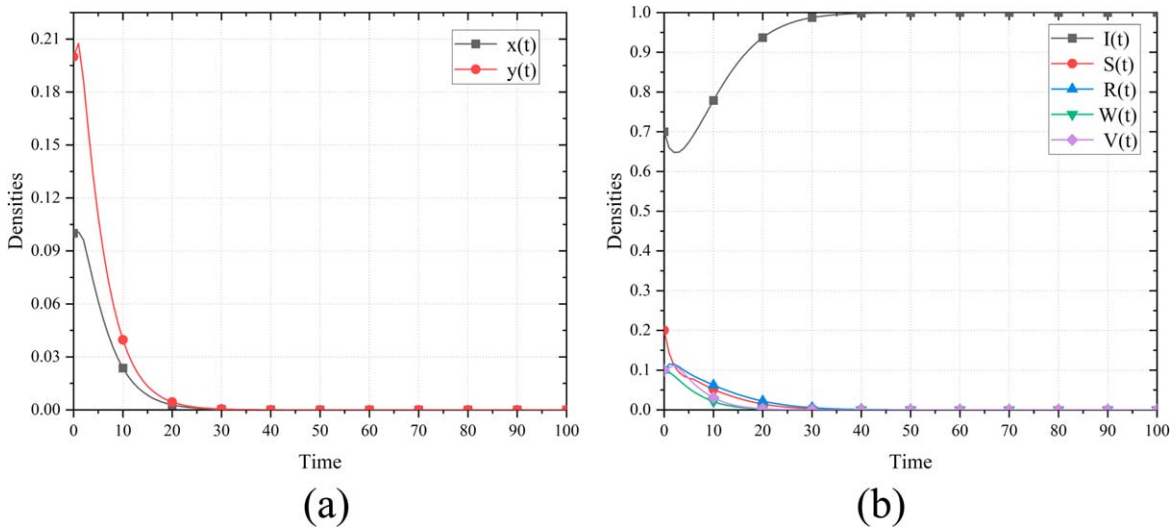

Figure 2. The stability of equilibrium E_1^0 of system (9).

$$
\begin{aligned}
&- Q_3Q_5Q_7\beta_3 I_7^* S_7^{*2} e^{-m_2\tau_2} + Q_4Q_8\beta_1\lambda I_7^* S_7^{*2} e^{-m_2\tau_2} \\
&+ Q_3Q_7\lambda^2\beta_3 I_7^* S_7^* e^{-m_2\tau_2} \\
&+ Q_5Q_7\beta_3\lambda I_7^* S_7^{*2} e^{-m_2\tau_2} + Q_1Q_3Q_5\lambda^2 S_7^* \\
&+ Q_2Q_5\lambda^2\beta_2 I_7^* S_7^* + Q_3Q_4\lambda^2\beta_1 I_7^* S_7^*
\end{aligned}
$$

$$
+ Q_2Q_8\beta_1\lambda I_7^* S_7^* x_7^* e^{-m_2\tau_2} + Q_2Q_5\lambda I_7^* S_7^* y_7^*\beta_3 e^{-m_2\tau_2},
$$

$$
\begin{aligned}
a_7 &= Q_1Q_3Q_5Q_8\lambda S_7^{*2} e^{-m_2\tau_2} \\
&+ Q_4Q_8\beta_1\beta_2\lambda I_7^{*2} S_7^{*2} e^{-m_1\tau_1 - m_2\tau_2} \\
&+ Q_5Q_7\beta_2\beta_3\lambda I_7^{*2} S_7^{*2} e^{-m_1\tau_1 - m_2\tau_2} \\
&+ Q_3Q_4Q_8\beta_1\lambda I_7^* S_7^{*2} e^{-m_2\tau_2} \\
&+ Q_3Q_5Q_7\beta_3\lambda I_7^* S_7^{*2} e^{-m_2\tau_2} \\
&- Q_2Q_5Q_8\beta_1\lambda I_7^* S_7^{*2} e^{-m_2\tau_2}.
\end{aligned}
$$

According to the Routh–Hurwith criterion, Routh table with at least one change of sign in the first column element, the polynomial has at least one right half-plane zero, so the internal equilibrium point E_7^* of the system is unstable. The proof is completed.

4. Numerical simulation

In this section, the correctness of the above theoretical results is verified by numerical simulations, and sensitivity analysis is done for important parameters. The comparison with the classical *ISR* model is made to confirm the superiority of the *ISRWVxy* model.

4.1. Stability simulation of equilibria for system

Example 1. Consider one of the scenarios of system (9): $\Lambda = 0.25$, $\lambda = 0.25$, $\beta_1 = 0.4$, $\beta_2 = 0.35$, $\beta_3 = 0.55$, $\alpha_1 = 0.2$, $\tau_1 = 5$, $\tau_2 = 1$, $b = 0.2$, $\varepsilon = 0.2$, $C_w = 10$, $C_v = 20$, $p = 0.4$, $\alpha = 0.2$, $\tau = 2$, $N = 1000$. By calculation, we get $R_0 = \dfrac{\beta_2\Lambda}{\lambda(\alpha_1+\lambda)e^{m_1\tau_1}} \approx 0.22 < 1$. From Theorem 1, we know that there exists a unique boundary rumor-free equilibrium point for system (9) when $R_0 < 1$. As shown in figure 2, the proportions x and y of spreaders uploading rumors in text form and rumors in video form tend to 0 as time goes on, and the density of the spreader tends to 0 indicating that the system eventually attains a stable state.

Example 2. Consider another scenario of system (9): $\Lambda = 0.2$, $\lambda = 0.19$, $\beta_1 = 0.45$, $\beta_2 = 0.2$, $\beta_3 = 0.55$, $\alpha_1 = 0.15$, $\tau_1 = 5$, $\tau_2 = 10$, $b = 0.2$, $\varepsilon = 0.2$, $C_w = 10$, $C_v = 20$, $p = 0.4$, $\alpha = 0.2$, $\tau = 10$, $N = 1000$. In this scenario, the calculation gives $R_1 = \dfrac{(\beta_1+\beta_2\lambda)\Lambda}{\lambda^2(\alpha_1+\lambda)e^{m_1\tau_1}} \approx 3.08 > 1$, $C_v < \dfrac{\beta_1 N\Lambda e^{-m_1\tau_1}}{\beta_1+\beta_2\lambda}\left(1-\dfrac{1}{R_1}\right) \approx 48.13$, which satisfies the condition in Theorem 2 (3), indicating that there is a boundary rumor epidemic equilibrium point in the system (9). As shown in figure 3, with the boundary conditions $x = 0$ and $y = 1$, the system eventually reaches a steady state, and the spreader persists in the system and do not die out, indicating that the rumor will always exist in the system.

Example 3. Consider the third scenario as, $\Lambda = 0.25$, $\lambda = 0.22$, $\beta_1 = 0.3$, $\beta_2 = 0.2$, $\beta_3 = 0.45$, $\alpha_1 = 0.12$, $\tau_1 = 5$, $\tau_2 = 1$, $b = 0.2$, $\tau_1 = 5$, $\tau_2 = 1$, $b = 0.2$, $\varepsilon = 0.2$, $C_w = 20$, $C_v = 10$, $p = 0.6$, $\alpha = 0.2$, $\tau = 10$, $N = 1000$. In this scenario, the calculation gives $R_2 = \dfrac{(\beta_3 e^{-m_2\tau_2}+\beta_2\lambda)\Lambda}{\lambda^2(\alpha_1+\lambda)e^{m_1\tau_1}} \approx 2.05 > 1$, $C_v < \dfrac{\beta_3 N\Lambda e^{-m_1\tau_1}}{\beta_3+\beta_2\lambda e^{m_2\tau_2}}\left(1-\dfrac{1}{R_3^0}\right) \approx 37.97$, and $\lambda I_6^* \approx 0.12 < \Lambda$, which satisfies the condition in Theorem 2 (4), indicating that there is a boundary rumor epidemic equilibrium point in the system. As shown in figure 4, with the boundary condition of $x = 1$, $y = 0$, the system eventually reaches the steady state and the spreader persist in the system and do not die out, indicating that the rumor will persist in the system.

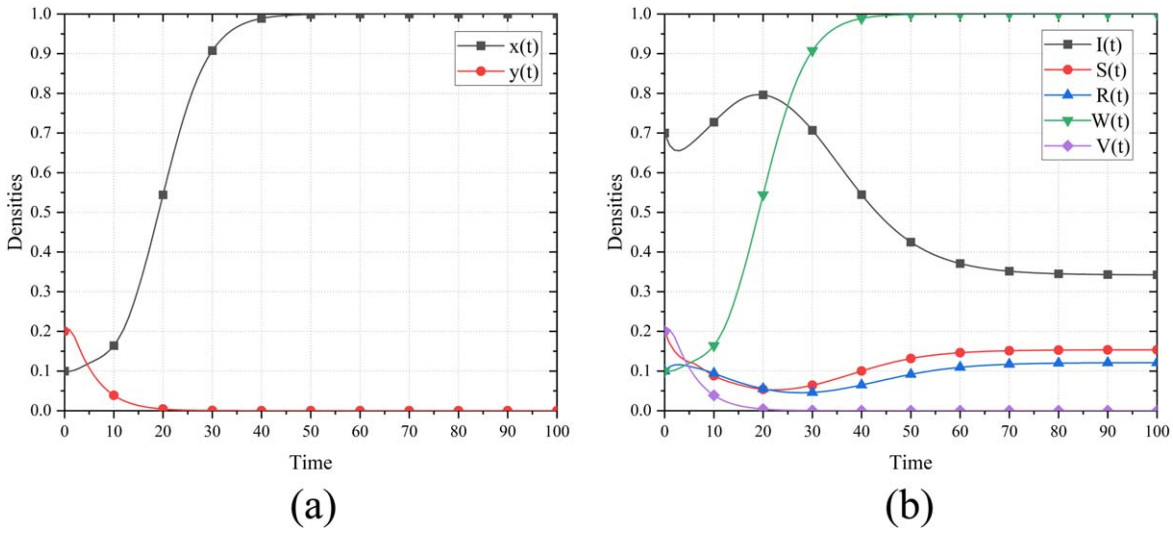

Figure 3. The stability of equilibrium E_5^* of system (9).

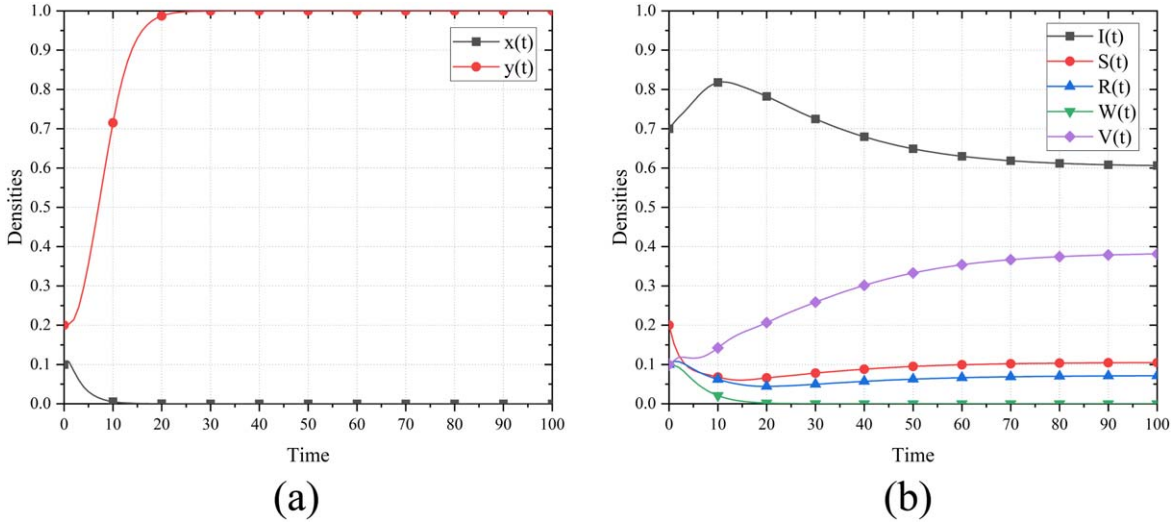

Figure 4. The stability of equilibrium E_6^* of system (9).

4.2. Sensitivity analysis

In system (9), it is evident that individual game behavior plays a crucial role in the rumor propagation process. When a spreader decides whether to post a text or video rumor in the information base, their attention is centered on their payoff. Therefore, we will separately simulate the impact of posting cost and time delay on the spreader's channel selection strategy separately.

Figure 5 illustrates the impact of the cost C_w for posting rumors in text form on the proportion of spreaders who choose this propagation strategy. The relevant parameters are detailed in table 3. As depicted by the black solid line in figure 5, when the cost C_w is low, the proportion of spreaders choosing the text information base propagation strategy gradually increases over time. As the propagation cost C_w increases, the proportion of spreaders favoring the text information base propagation strategy decreases accordingly but still experiences an upward trend, as indicated by the red

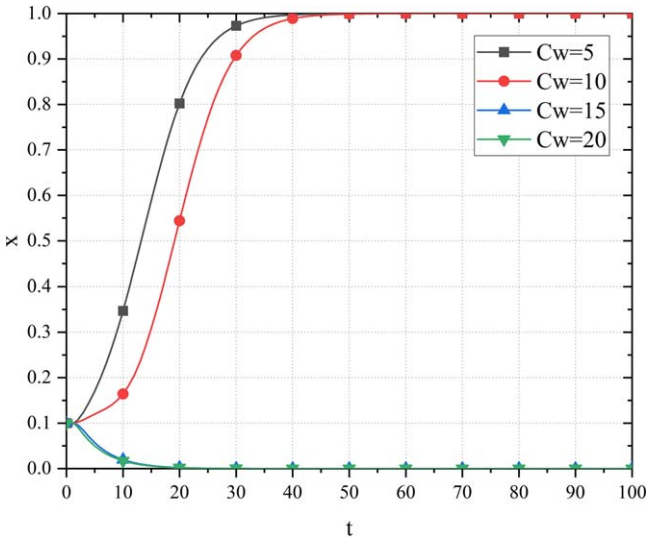

Figure 5. The densities evolution of spreaders with different C_w.

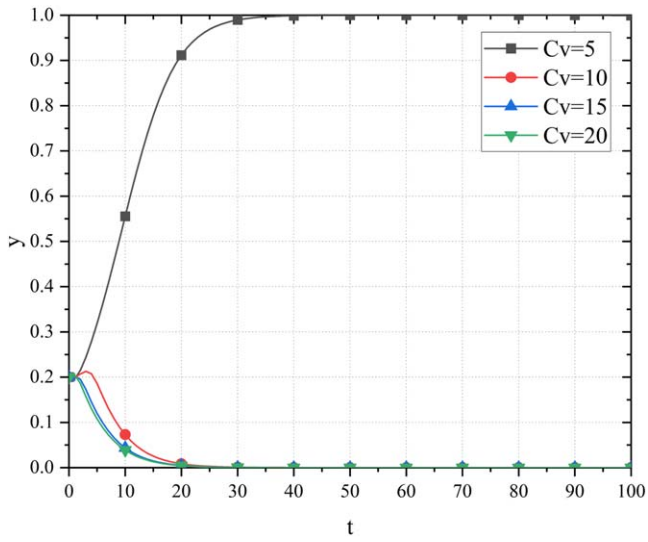

Figure 6. The density evolution of spreaders with different C_v.

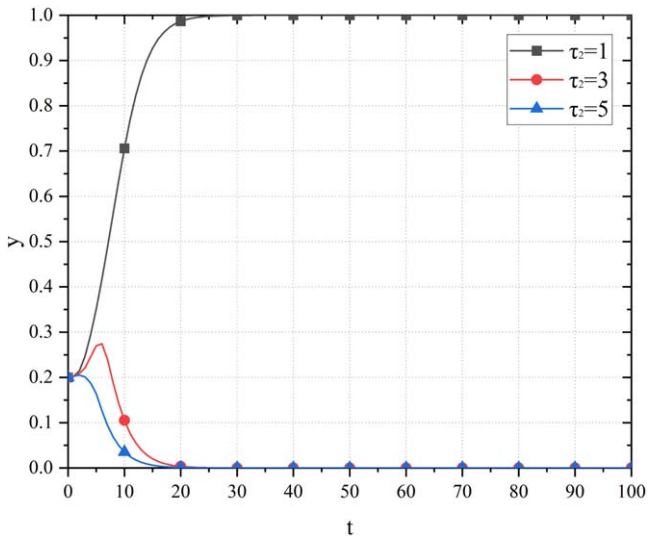

Figure 7. The density evolution of video spreaders with different τ_2.

Table 3. Parameter for text spreaders.

Symbol	Value	Symbol	Value
Λ	0.2	b	0.2
λ	0.19	ε	0.2
β_1	0.45	C_w	5,10,15,20
β_2	0.2	C_v	20
β_3	0.55	p	0.4
α_1	0.15	α	0.2
τ_1	5	τ	10
τ_2	10	N	1000

Table 4. Parameter for rumor spreaders.

Symbol	Value	Symbol	Value
Λ	0.2	b	0.2
λ	0.19	ε	0.2
β_1	0.45	C_w	10
β_2	0.2	C_v	5,10,15,20
β_3	0.55	p	0.4
α_1	0.15	α	0.2
τ_1	5	τ	10
τ_2	10	N	1000

solid line in figure 5. With further increases in cost, the proportion of spreaders who choose the text information propagation strategy becomes smaller and eventually diminishes to zero, as demonstrated by the blue solid line and the green solid line in figure 5. It is noteworthy that the difference between the green solid line and the blue solid line is marginal, indicating that when the cost becomes sufficiently high, the choice of strategy by spreaders becomes insensitive to cost variations.

Figure 6 simulates the impact of the cost C_v for uploading rumors in video form on the proportion y of spreaders who choose this propagation strategy. The relevant parameter settings are provided in table 4. Similar to figure 5, in general, the magnitude of the proportion y of spreaders choosing the video information base propagation strategy is inversely proportional to the magnitude of the cost paid C_v. However, unlike the trend depicted in figure 5, when $C_v = 10$, the proportion y of spreaders who choose the video information base propagation strategy decreases over time. This phenomenon indicates that the proportion y of spreaders choosing video information base propagation strategy is more sensitive to the change in the cost C_v during this period. Notably, there is minimal distinction between the solid blue line and the solid green line, suggesting that y becomes less sensitive to cost fluctuations as the cost attains a sufficiently high level.

By comparing figure 5 with figure 6, we find that when the cost of the strategies are both ten, the proportion of spreaders choosing the strategy of text information base channel x still continues to increase, while the proportion of spreaders choosing the strategy of video information base channel y decreases to zero, which indicates that the spreaders are more sensitive to C_v. Therefore, in formulating strategies to deal with rumor propagation, the management department needs to pay more attention to the management and monitoring of the text database channel, and formulate corresponding policies for C_v, so as to achieve better control effects with smaller control costs, and thus achieve more accurate rumor management. This kind of management strategy is expected to play a positive role in the actual response to rumor propagation.

Figure 7 simulates the time-evolution plot of the proportion of the spreaders who choose the video message bank to spread rumors at time delays $\tau_2 = 1$h, 3h, 5h. The relevant parameters are set as shown in table 5. As can be seen in figure 7, time delay τ_2 is negatively correlated with the proportion y of spreaders posting video rumors. When $\tau_2 = 1$h, the proportion y exhibits an increasing trend over time. However, as τ_2 increases to 3h, y shows a trend of initially rising and subsequently declining with time until it becomes 0. When τ_2 further increases to 5h, y steadily decreases with

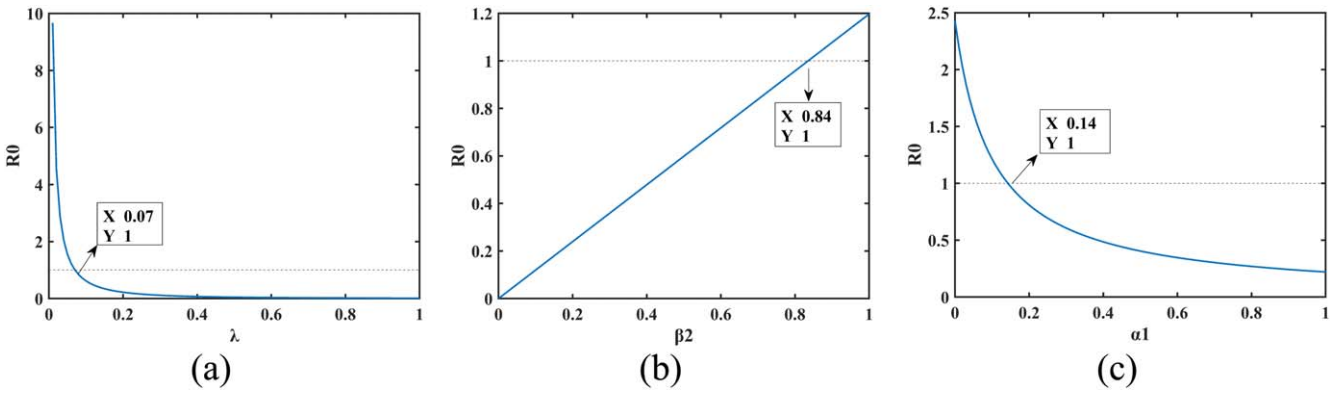

Figure 8. Parameter for λ, β_2 and α_1 for R_0.

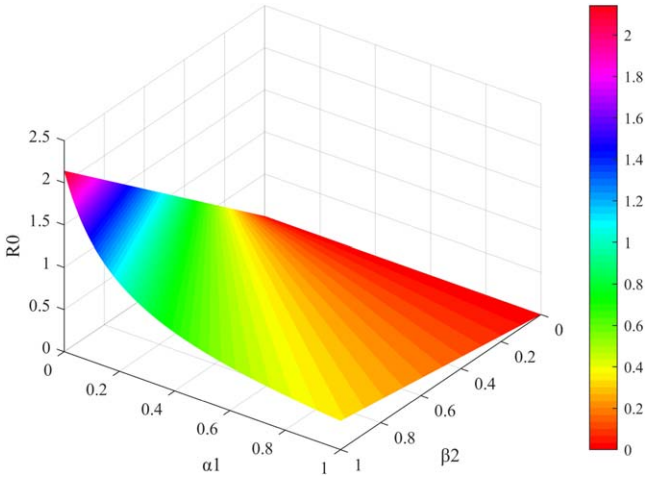

Figure 9. The relation among β_2, α_1 and R_0.

Table 5. Parameter for video spreaders.

Symbol	Value	Symbol	Value
Λ	0.2	b	0.2
λ	0.19	ε	0.2
β_1	0.45	C_w	10
β_2	0.2	C_v	20
β_3	0.55	p	0.4
α_1	0.15	α	0.2
τ_1	5	τ	10
τ_2	1,3,5	N	1000

time. This indicates that the longer it takes for spreaders to produce videos, the smaller the proportion of spreaders choosing the information base propagation strategy. Therefore, in the real rumor propagation process, officials can implement stricter video posting requirements to extend the time delay in video rumor production. This strategic approach can effectively reduce the scale of rumor propagation and mitigate the negative impact of rumors.

In addition to analyzing the impact of the above factors on rumor propagation, the basic regeneration number R_0 is a very important indicator in the rumor propagation process. It

Table 6. Parameter for the basic reproduction number.

Symbol	Value	Symbol	Value
Λ	0.2	b	0.2
λ	0.19	ε	0.2
β_1	0.45	C_w	10
β_2	[0–1]	C_v	20
β_3	0.55	p	0.4
α_1	[0–1]	α	0.2
τ_1	5	τ	10
τ_2	10	N	1000

can measure the rumor propagation ability. The larger the value of R_0, the stronger the rumor propagation ability, i.e., the more difficult the rumor is to be controlled. Therefore, it is very important to study the factors influencing the value of R_0. In this subsection, we simulate the effects of removal rate λ, propagation rate β_2, and recovery rate α_1 on the value of R_0.

The effects of parameters λ, β_2 and α_1 on R_0 are simulated in figure 8, respectively. In figure 8(a), we can see that the basic regeneration number R_0 and the removal rate λ are negatively correlated, i.e., R_0 decreases with the increase of the removal rate λ. This observation implies that a higher removal rate weakens the rumor's propagation ability, and when the removal rate is sufficiently high, R_0 diminishes to zero. Figure 8(b) reveals that as the propagation rate β_2 increases, R_0 also increases. This trend indicates that a higher propagation rate enhances the rumor's propagation potential, leading to increased difficulty in controlling it. Finally, figure 8(c) demonstrates a negative correlation between R_0 and the recovery rate α_1. As the recovery rate α_1 increases, the basic regeneration number R_0 decreases, indicating that the faster the rate at which people forget or lose interest in the rumor, the weaker the rumor propagation ability.

Figure 9 simulates the relation among the basic regeneration number R_0, α_1 and β_2. The relevant parameters are set as shown in table 6. From figure 9, we observe two noteworthy aspects. Firstly, as the propagation rate β_2 increases, the basic regeneration number R_0 also increases, which is consistent with the trend in figure 8(b). However, the extent to

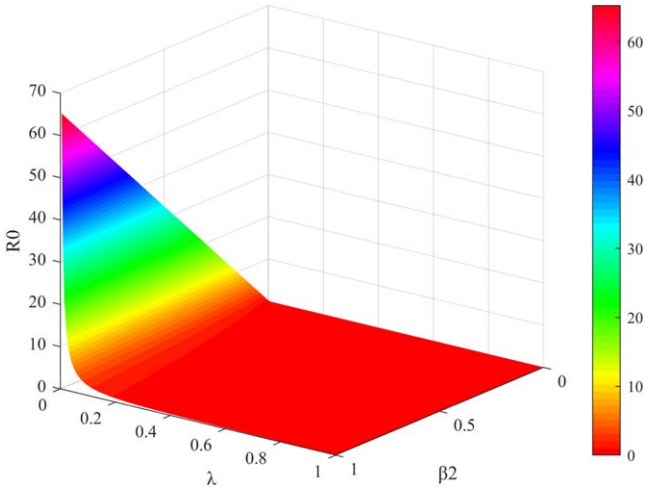

Figure 10. The relation among β_2, λ and R_0.

Table 7. Parameter for the basic reproduction number.

Symbol	Value	Symbol	Value
Λ	0.2	b	0.2
λ	[0–1]	ε	0.2
β_1	0.45	C_w	10
β_2	[0–1]	C_v	5,10,15,20
β_3	0.55	p	0.4
α_1	0.15	α	0.2
τ_1	5	τ	10
τ_2	10	N	1000

which changes in β_2 affect R_0 varies with the value of α_1. Specifically, for larger values of α_1, changes in β_2 have a relatively minor impact on R_0. Conversely, for smaller values of α_1, R_0 becomes more sensitive to variations in β_2, with even slight changes in β_2, resulting in substantial fluctuations in R_0. Secondly, the basic regeneration number R_0 is negatively correlated with the recovery rate α_1, aligning with figure 8(c). Similarly, the influence of changes in α_1 on R_0 is determined by the specific value of β_2. When β_2 is small, alterations in α_1 have a relatively modest effect on R_0. Conversely, when β_2 is larger, R_0 becomes more sensitive to the changes in α_1.

Figure 10 simulates the relation among the basic regeneration number R_0, λ and β_2. The relevant parameter settings are shown in table 7. As depicted in figure 10, R_0 is negatively correlated with λ, which is in line with the results in figure 8(a). Notably, β_2 has a relatively small effect on this correlation trend. It's worth emphasizing that when λ exceeds 0.5, changes in β_2 have little impact on R_0. This underscores the significance of the removal rate λ as a critical system parameter. When λ reaches a sufficiently high value, regardless of how the propagation rate fluctuates, the basic reproduction number R_0 remains at zero. This implies that rumors cannot propagate on a large scale. Consequently, this finding suggests that enhancing the removal rate through measures such as blocking, deletion, and bans can be an effective strategy for controlling the widespread propagation of rumors.

In figures 9 and 10, the Z-axis both denote R_0, the X-axis both denote β_2, while the Y-axis denote α_1 and λ, respectively. comparing the Y-axis of the two figures, it can be seen that the rate of change of the surface along the λ-direction is greater in figure 9, which suggests that λ has a more significant effect on R_0. In other words, it is more efficient to increase the removal rate in controlling rumor propagation. This suggests that the relevant departments should focus on strengthening the management and control of information sources when formulating countermeasures. By means of gagging and other means, it is more likely to achieve significant results, effectively curbing the rise of R_0 and thus controlling the spread of rumors more efficiently.

5. Model application with a real dataset

In this section, we use a real dataset to evaluate the effectiveness of the model in this paper. The data is sourced from real Twitter datasets [43], which encompass information on 12 distinct rumors, spanning from the inception of each rumor to its cessation, encompassing both original tweets and retweeted content. From this set of 12 rumors, we identified the dataset with the most extensive volume of data, which is referred to as dataset 12 in this paper.

The dataset documents that the propagation dynamics of the rumor titled 'A screenshot from MyLife.com confirms that mail bomb suspect Cesar Sayoc was registered as a Democrat'. As shown in table 8, each column within the dataset contains specific information related to individual tweets and retweets. This information includes user IDs, timestamps corresponding to the date and time of each tweet or retweet, tweet statuses, and other pertinent details. Tweets marked with the status 'r' are categorized as rumor tweets, with the corresponding user IDs serving as the spreaders in the model proposed in this paper.

Subsequently, we performed data preprocessing on the 32,083 pieces of data from 0–76 h, eliminating data segments such as missing IDs, timestamp anomalies, etc., and finally obtained 14,931 cleaned data. Based on this cleaned data, we choose the whole data with state r as the dataset for the neural network algorithm. Specifically, we use the neural network algorithm on the TensorFlow platform to process the data from 0 to 76 h, taking the data from 0–36 h as the training set, and the data from 37–76 h as the validation set. A set of more desirable parameters is finally obtained, as shown in table 9. With this set of parameters, we can better fit the dynamic characteristics of actual rumor spreading.

Figure 11(a) shows the fitting effect between the first 36 h actual data and the model, and it can be seen that the model can fit the trajectory of the actual data well. Subsequently, the parameters listed in table 9 were employed to forecast the rumor's progression within the framework of this paper's model. The prediction results are depicted as dotted lines in figure 11(b). Finally, we employed the last 40 h of data from the authentic dataset to validate the predictive

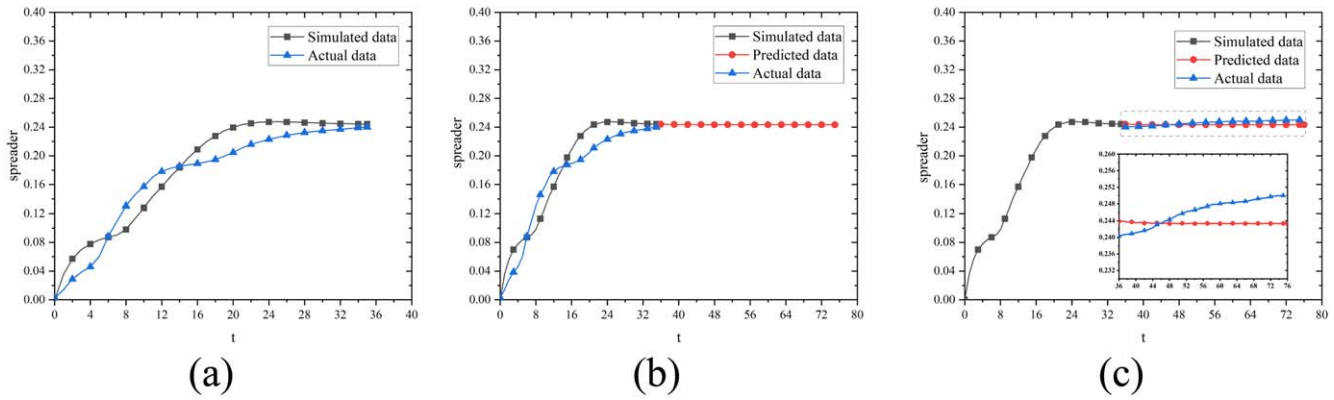

Figure 11. The spreader density curve of the model and actual data curve.

Table 8. Dataset 12 from the Twitter real datasets.

ID	Date & Time	···	Followers	State of Tweet
20414250	['2018', 'Oct', '29', '20:03:27']	···	382	r
930195128	['2018', 'Oct', '29', '20:03:10']	···	5457	r
45090008	['2018', 'Oct', '29', '20:00:11']	···	96	a
1048362827201880000	['2018', 'Oct', '29', '19:59:46']	···	229	r
819942782903009000	['2018', 'Oct', '29', '19:59:13']	···	26	r
...	...	...	...	...
822430183261110000	['2018', 'Oct', '29', '19:51:28']	···	1185	r
894929166	['2018', 'Oct', '29', '19:47:58']	···	33	r

Table 9. Parameter for the model validation.

Symbol	Value	Symbol	Value
Λ	0.19	b	0.001
λ	0.15	ε	0.2
β_1	0.33	C_w	10
β_2	0.32	C_v	20
β_3	0.47	p	3.9
α_1	0.25	α	0.99
τ_1	3	τ	10
τ_2	10	N	1000

accuracy of the model, as illustrated in figure 11(c). The results affirm the model's robust performance in anticipating rumor propagation dynamics, effectively emulating real-world propagation processes. This not only proves the feasibility and accuracy of the model, but also provides a powerful tool for us to gain a deeper understanding of the mechanism of rumor propagation.

Leveraging these findings, we can employ the model for rumor detection, early warning, and timely response, enabling us to proactively manage and mitigate the spread and impact of rumors. This represents a substantial step toward fostering a more harmonious online environment and holds significant practical application value.

Furthermore, we conducted a comparative analysis between the prediction results generated by the model presented in this paper and the classical *ISR* model, as illustrated in figure 12. The comparative examination reveals that both the peak spreader density and the final spread size in the *ISRWVxy* propagation model surpasses those in the traditional *ISR* model. This discrepancy indicates that rumors propagate more extensively in the context of multi-channel propagation. Moreover, it's notable that the *ISRWVxy* model attains its peak propagation earlier than the traditional *ISR* model, indicating a faster rumor propagation rate in the multi-channel framework. Then, we use Python to evaluate the fitting results of the two models with real data respectively, and the evaluation results are shown in table 10. R-squared, RMSE (Root Mean Squared Error) and MAE (Mean Absolute Error) are used as evaluation indexes in the comparison experiment. A higher R-squared value indicates a better model fit, while a lower RMSE signifies closer alignment between predicted and actual values. Additionally, a smaller MAE value indicates improved prediction accuracy. From the experimental outcomes detailed in table 10, it is evident that the *ISRWVxy* model outperforms the *ISR* model. The *ISR* model, which only takes into account the individual interactive communication, exhibits substantial errors when simulating real-world scenarios. In contrast, the multi-channel rumor propagation model, which incorporates information base propagation, more accurately mirrors the dynamics of rumor propagation. As a result, the model introduced in this paper holds the potential to offer valuable guidance for real-world rumor control efforts.

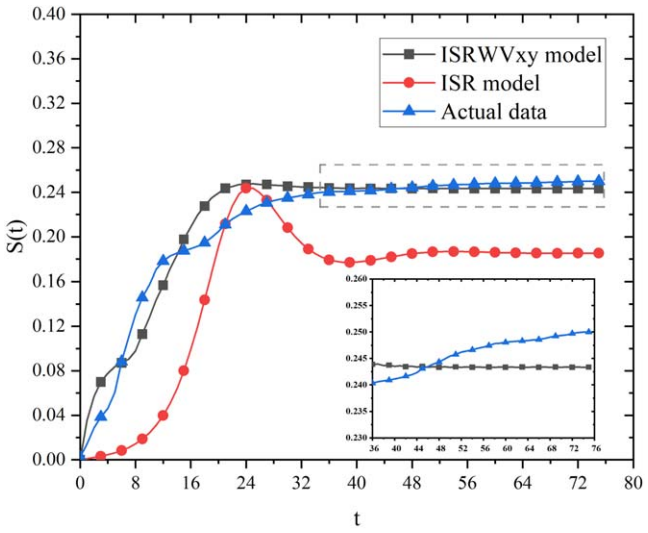

Figure 12. Comparison of *ISRWVxy*, *ISR* and the actual data.

Table 10. Evaluation index.

Model	R-squared	RMSE	MAE
ISRWVxy	0.9365	0.0158	0.0113
ISR	−0.1449	0.0667	0.0590

6. Conclusion

In this paper, a multi-channel rumor propagation model including propagation of individuals game strategy and time delay was proposed. Firstly, the basic regeneration number was derived using the next generation matrix method, and six boundary equilibria and one internal equilibria of the system were obtained. Secondly, the local asymptotic stability of the seven equilibrium points was proved by using Routh–Hurwitz judgment, and Descartes' Rule of Signs. Subsequently, the above theoretical results were verified by numerical simulations. The results indicated that as the cost of propagation increases, the likelihood that a spreader chooses an online propagation strategy during the game decreases. This trend is more evident in the video information base channel strategy. This insight suggests that regulatory authorities can effectively curb rumor spreading by increasing the associated propagation costs. Furthermore, we analyzed the sensitivity of the threshold R_0 and found that the thresholds increase as the propagation rate rises. Meanwhile, the effect of the removal rate on the threshold is more obvious, and the regulatory authority can control the rumor more precisely by blocking and banning. Finally, we validated the model's effectiveness through the utilization of a real Twitter dataset. Moreover, experimental comparison with the classical *ISR* model conclusively demonstrated the superiority of the proposed *ISRWVxy* model in terms of performance and accuracy.

In summary, the multi-channel rumor propagation model, along with the theoretical analysis, numerical simulation and real data validation, provides some useful insights for rumor control and mitigation efforts. By considering factors such as propagation costs, time delay, propagation rate and removal rate that affect rumor propagation, the model in this paper helps to facilitate a more informed and prepared response to rumor propagation in contemporary society.

Acknowledgments

This work was partially supported by the Project for the National Natural Science Foundation of China (72174121, 71774111), and the Program for Professor of Special Appointment (Eastern Scholar) at Shanghai Institutions of Higher Learning, and the Project for the Natural Science Foundation of Shanghai (21ZR1444100).

Competing interests

The authors declare that they have no competing interests.

References

[1] Kemp S 2023 Digital 2023 July Global Statshot Report https://datareportal.com/reports/digital-2023-july-global-statshot
[2] Guo H and Yan X 2023 Dynamic modeling and simulation of rumor propagation based on the double refutation mechanism *Inf. Sci.* **630** 385–402
[3] Zhang Y and Zhu L 2023 Modeling the dynamics of information propagation in the temporal and spatial environment *Commun. Theor. Phys.* **75** 095002–095002
[4] Zhang Z, Mei X, Jiang H, Luo X and Xia Y 2023 Dynamical analysis of Hyper-SIR rumor spreading model *Appl. Math. Comput.* **446** 127887–127887
[5] Li Z, Zhang Q, Du X, Ma Y and Wang S 2021 Social media rumor refutation effectiveness: Evaluation, modelling and enhancement *Inf. Process. Manage.* **58** 102420
[6] Maia H P, Ferreira S C and Martins M L 2023 Controversy-seeking fuels rumor-telling activity in polarized opinion networks *Chaos, Solitons Fractals* **169** 113287–113287
[7] Dong S and Huang Y-C 2018 A class of rumor spreading models with population dynamics *Commun. Theor. Phys.* **70** 795
[8] Wang X, Li Y, Li J, Liu Y and Qiu C 2021 A rumor reversal model of online health information during the Covid-19 epidemic *Inf. Process. Manage.* **58** 102731
[9] Xiang T, Li Q, Li W and Xiao Y 2023 A rumor heat prediction model based on rumor and anti-rumor multiple messages and knowledge representation *Inf. Process. Manage.* **60** 103337
[10] Hoang M T 2023 Lyapunov functions for studying global asymptotic stability of two rumor spreading models *Commun. Theor. Phys.* **75** 105802
[11] Wang C, Liu R and Wang Y 2023 The spread dynamics model of the interaction between rumors and derivative rumors in emergencies under the control strategy *Chaos, Solitons Fractals* **175** 114062–114062
[12] Li J, Jiang H, Mei X, Hu C and Zhang G 2020 Dynamical analysis of rumor spreading model in multi-lingual environment and heterogeneous complex networks *Inf. Sci.* **536** 391–408

[13] Yu S, Yu Z, Jiang H, Mei X and Li J 2020 The spread and control of rumors in a multilingual environment *Nonlinear Dyn.* **100** 2933–51
[14] Yu S, Yu Z, Jiang H and Yang S 2021 The dynamics and control of 2I2SR rumor spreading models in multilingual online social networks *Inf. Sci.* **581** 18–41
[15] Yin F, Jiang X, Qian X, Xia X, Pan Y and Wu J 2022 Modeling and quantifying the influence of rumor and counter-rumor on information propagation dynamics *Chaos, Solitons Fractals* **162** 112392
[16] Zhu L, Liu W-S and Zhang Z 2020 Delay differential equations modeling of rumor propagation in both homogeneous and heterogeneous networks with a forced silence function *Appl. Math. Comput.* **370** 124925–124925
[17] Li J, Jiang H, Yu Z and Hu C 2019 Dynamical analysis of rumor spreading model in homogeneous complex networks *Appl. Math. Comput.* **359** 374–85
[18] Huo L and Dong Y 2020 Analyzing the dynamics of a stochastic rumor propagation model incorporating media coverage *Math. Methods Appl. Sci.* **43** 6903–20
[19] Huo L, Chen X and Zhao L 2023 The optimal event-triggered impulsive control of a stochastic rumor spreading model incorporating time delay using the particle swarm optimization algorithm *J. Franklin Inst.* **360** 4695–718
[20] Li M, Zhang H, Georgescu P and Li T 2021 The stochastic evolution of a rumor spreading model with two distinct spread inhibiting and attitude adjusting mechanisms in a homogeneous social network *Physica A* **562** 125321
[21] Jain A, Dhar J and Gupta V 2019 Stochastic model of rumor propagation dynamics on homogeneous social network with expert interaction and fluctuations in contact transmissions *Physica A* **519** 227–36
[22] Huo L, Dong Y and Lin T 2021 Dynamics of a stochastic rumor propagation model incorporating media coverage and driven by Lévy noise* *Chin. Phys.* B **30** 080201
[23] Wang Z, Xia C, Chen Z and Chen G 2020 Epidemic Propagation With Positive and Negative Preventive Information in Multiplex Networks *IEEE Transactions on Cybernetics* **51** 1454–62
[24] Wang Z, Guo Q, Sun S and Xia C 2019 The impact of awareness diffusion on SIR-like epidemics in multiplex networks *Appl. Math. Comput.* **349** 134–47
[25] Wang J, Jiang H, Ma T and Hu C 2019 Global dynamics of the multi-lingual SIR rumor spreading model with cross-transmitted mechanism *Chaos, Solitons Fractals* **126** 148–57
[26] Zhang Y, Su Y, Weigang L and Liu H 2019 Interacting model of rumor propagation and behavior spreading in multiplex networks *Chaos, Solitons Fractals* **121** 168–77
[27] Song Z, Zhen B and Hu D 2020 Multiple bifurcations and coexistence in an inertial two-neuron system with multiple delays *Cognitive Neurodynamics* **14** 359–74
[28] Song Z, Xu J and Zhen B 2019 Mixed-coexistence of periodic orbits and chaotic attractors in an inertial neural system with a nonmonotonic activation function *Mathematical Biosciences and Engineering* **16** 6406–25
[29] Cheng Y, Huo L and Zhao L 2021 Dynamical behaviors and control measures of rumor-spreading model in consideration of the infected media and time delay *Inf. Sci.* **564** 237–53
[30] Zhu L and Huang X 2019 SIS model of rumor spreading in social network with time delay and nonlinear functions *Commun. Theor. Phys.* **72** 015002
[31] Jia P, Wang C, Zhang G and Ma J 2019 A rumor spreading model based on two propagation channels in social networks *Physica*A **524** 342–53
[32] Dong Y, Huo L and Zhao L 2022 An improved two-layer model for rumor propagation considering time delay and event-triggered impulsive control strategy *Chaos, Solitons Fractals* **164** 112711
[33] Shao Q, Xia C, Wang L and Li H-J 2019 A new propagation model coupling the offline and online social networks *Nonlinear Dyn.* **98** 2171–83
[34] Guan G and Guo Z 2021 Stability behavior of a twosusceptibility SHIR epidemic model with time delay in complex networks *Nonlinear Dyn.* **106** 1083–110
[35] Xiao Y, Chen D, Wei S, Li Q, Wang H and Xu M 2018 Rumor propagation dynamic model based on evolutionary game and anti-rumor *Nonlinear Dyn.* **95** 523–39
[36] Askarizadeh M, Tork Ladani B and Manshaei M H 2019 An evolutionary game model for analysis of rumor propagation and control in social networks *Physica A* **523** 21–39
[37] Li Q, Xiang T, Dai T and Xiao Y 2023 An information dissemination model based on the Rumor & Anti-Rumor & stimulate-rumor and tripartite cognitive game *IEEE Transactions on Cognitive and Developmental Systems* **15** 925–37
[38] Mei J, Wang S, Xia D and Hu J 2022 Global stability and optimal control analysis of a knowledge transmission model in multilayer networks *Chaos, Solitons Fractals* **164** 112708–112708
[39] Dong Y, Huo L, Xie X and Li M 2023 An improved ISR-WV rumor propagation model based on multichannels with time delay and pulse vaccination *Chin. Phys.* **32** 070205–070205
[40] Fu F, Rosenbloom D I, Wang L and Nowak M A 2011 Imitation dynamics of vaccination behaviour on social networks *Proceedings of the Royal Society B: Biological Sciences* **278** 42–9
[41] Zhang H, Fu F, Zhang W and Wang B 2012 Rational behavior is a 'double-edged sword' when considering voluntary vaccination *Physica A* **391** 4807–15
[42] Ge J and Wang W 2022 Vaccination games in prevention of infectious diseases with application to COVID-19 *Chaos, Solitons Fractals* **161** 112294–112294
[43] Amirhosein B 2019 Newly Emerged Rumors in Twitter https://zenodo.org/records/2563864